Supplementary Information

Edwards et *al*. PNAS

Soil collection for greenhouse experiment and microbiome acquisition experiment

Soil from the rice field in Sacramento (38.58575 degrees north and -121.596911 West) was collected on 3/15/2013 using shovels to gather down to a depth of approximately 8 inches. Soil from the rice field in Arbuckle, CA (39.011732 degrees North and -121.92212 degrees West) was collected on 3/18/2013 using a front-end loader to gather down to a depth of approximately 8 inches. Soil from a rice field in Davis, CA (38.543864 degrees North and -121.81223 West) was collected on 3/19/2013 using shovels to gather down to a depth of approximately 8 inches. All soils were transported back to the greenhouse and stored until planting on 3/28/2013. All soils were mixed individually in clean tubs to homogenize the soil. The soil was placed into new 5 x 5 inch pots that were then placed into tubs (24 pots each). Each tub contained only one soil type in order to avoid microbial mixing between the soils. Each tub was watered in order to submerge the soils as suited to rice cultivation. Soil from the Davis field was collected for the microbiome acquisition experiment on 11/26/2013 using the same method as described above. Soil samples for the Arbuckle, Davis, and Sacramento fields were analyzed at the UC Davis Analytical Lab for chemical content (Dataset S8).

Plant germination, transplantation, and cultivation in the greenhouse and microbiome acquisition experiment

Seeds from 6 cultivated varieties (M104, Nipponebare, IR50, 93-11, TOg 7102, and TOg 7267) were dehulled, surface sterilized in 70% bleach for 5 minutes and sterilely germinated on MS agar media in the dark. After germination, the rice seedlings were transplanted into the various soils in the greenhouse. The tubs were watered every other day and nutrients were supplied to each tub on 2-week basis on 4/12/2013 and 4/26/2013. All weeds were manually removed from the pots when identified.

For the microbiome acquisition experiment, M104 seeds were dehulled and surface sterilized in bleach for 5 minutes and subsequently germinated on MS agar media in the dark. The seedlings were transplanted into Davis soil in the greenhouse and sampled according to the time series using the same protocol for sample collection detailed above.

Experimental design for greenhouse and microbiome acquisition experiments

The greenhouse experiment was designed as a split-split plot experiment. Briefly, there were 12 tubs total so that each soil had 4 tubs. We collected only one rhizocompartment from each pot such that each every rhizocompartment was taken from every cultivar once per tub, giving a total of 18 rhizocompartment samples and 6 bulk soil samples per tub (Dataset S1). Because the selected cultivars flower at various times, to avoid confounding issues between developmental stages and cultivar effects we collected all samples at 42 days while all cultivars were still vegetatively growing.

The plants for the acquisition experiment were all contained in one large tub along with unplanted pots for bulk soil controls. Each plant collected had all three rhizocompartments sampled.

Experimental design of the field experiment

All fields sampled in the field experiment are managed by Lundberg Family Farms (Richvale, CA, USA). All of these fields are subject to typical California rice cultivation practices (presoaked seeds, aerial seeding, dense planting, etc), with the cultivation differences being between “eco farming” and organic farming of the fields. 8 individual plants were sampled per field site (Dataset S1).

Sample Collection of Rhizosphere, Rhizoplane, and Endosphere Fractions

Samples were collected over a 4-day period from 5/6/2013 to 5/9/2013. The soil and plant were removed from each pot and the roots were removed from the soil. We avoided collecting any roots that were at the interface of the pot and the soil in order to avoid false environments. The excess soil was manually shaken from the roots, leaving approximately 1mm of soil still attached to the roots (Fig. S2). We separated the 1mm of soil from the roots directly in the greenhouse by placing the roots with soil still attached in a sterile flask with 50 ml of sterile Phosphate Buffered Saline (PBS) solution. The roots were then stirred vigorously with sterile forceps in order to clean all the soil from the root surfaces. The soil

that was cleaned from the roots was poured into a 50ml Falcon tube and stored as the rhizosphere compartment at 4°C until DNA extraction the same day.

The roots designated for rhizoplane collection were cleaned in the greenhouse and placed in a Falcon tube with 15 ml PBS, and tightly adhering microbes at the root surface were removed using a sonication protocol originally developed for Arabidopsis roots (1-3). The roots in the Falcon tube were sonicated for 30 s at 50-60 Hz (output frequency 42 kHz, power 90 W, Branson Unltrasonics). The sonication procedure strips the rhizoplane microbes from the root surface as well as portions of the rhizodermis as evidenced by the gradient of organellar reads from the rhizoplane to the endosphere (Fig. S27). The roots were then removed and discarded and the liquid PBS fraction was kept as the rhizoplane compartment.

The roots designated for the endosphere collection were cleaned and sonicated as described before. Two more sonication procedures using clean PBS solution were used to ensure that all microbes were removed from the root surface. CARD-FISH on whole non-sonicated roots and thrice sonicated roots was used to analyze the efficacy of this procedure for removing microbes from the rhizoplane (Fig. S3). The sonicated roots were then stored at -80°C until DNA extraction the same day.

Bulk soil samples were collected from unplanted pots approximately 2 inches below the soil surface. The samples were placed in 15 ml tubes and stored at 4°C until DNA extraction the same day.

Samples for the field experiment were collected over a two-day period. The roots of plants in the field were collected with a bulb planter (Fiskars). The soil was shaken off the roots to leave ~1mm of soil still attached. These roots were placed in sterile PBS solution and brought back to the laboratory for isolation of the rhizocompartments as described above. Each rhizocompartment was isolated from each plant sampled and had total DNA extracted.

DNA Extraction from Rhizocompartments

The rhizosphere soil was concentrated by pipetting 1mL of the PBS / rhizosphere soil into a 2mL tube and centrifuging for 30 seconds at 10,000 g. The supernatant was discarded leaving only the soil fraction behind. The rhizoplane compartment was concentrated in the same manner, except all 15mL of

77 the sample was concentrated in the same 2 mL tube using multiple centrifugations. The endosphere
78 fraction was pre-homogenized before the DNA extraction by bead beating for 1 minute (Mini Beadbeater,
79 Biospec Products). The DNA for each sample was then extracted using the MoBio PowerSoil DNA
80 isolation kit and eluted in 50 µL of elution buffer. The rhizoplane samples typically had low DNA yield
81 and were subsequently concentrated in a speedvac down to 10 µL.

82 **16S rRNA gene V4 amplification, quantitation, and sequencing**

83 Targeted metagenomic profiling of the samples was carried out by sequencing the V4 region of
84 the 16S rRNA gene. V4 amplification was carried out using primers modified from Caporaso et al, 2010
85 (4). Briefly, these primers are designed to amplify from 515 to 806 of the 16S rRNA gene and they
86 include a barcode an adaptor for annealing to the Illumina flow cell. Our primers differed in that both the
87 primers contained a 12bp barcode instead of only the reverse primer (Dataset S25). This allowed us to
88 pool many samples together using unique barcode combinations instead of relying on a multitude of
89 reverse primers with unique barcodes. PCR reaction mixes were made using Qiagen HotStar HiFidelity
90 polymerase. Each mix was done in a volume of 25 µL using 14 µL H_2O, 5 µL HotStar PCR Buffer, 2.5
91 µL forward primer (10 µM), 2.5 µL reverse primer (10 µM), 1 µL sample DNA, and 0.5 µL HotStar
92 polymerase. We used a touchdown PCR program on a Biometra TProfessional Basic Gradient
93 thermocycler: 95°C for 5 min, then 7 cycles of 95°C for 45 sec, 65°C for 1 min (decreasing at 2°C /
94 cycle), and 72°C for 90 sec, followed by 30 cycles of 95°C for 45 sec, 50°C for 30 sec, and 72°C for 90
95 sec. A final extension at 72°C was used for 10 min and the reactions were held at 4°C. The reactions
96 were run on a 1% agarose gel in order to ensure the amplification was successful. Unsuccessful reactions
97 were attempted once more, but removed from the experiment if unsuccessful a second time.

98 The amplicons libraries were diluted 40x and quantified using an Agilent Bioanalyzer for the
99 greenhouse libraries, or a Caliper LabChip GX for the field experiment libraries at the DNA Technologies
100 Core at the Genome Center, UC Davis. The libraries were then pooled at equimolar concentrations into 4
101 pooled libraries (2 libraries for the greenhouse experiment and 2 libraries for the field experiment). To
102 remove any primer dimer from the pooled amplicon libraries we ran the 4 pooled libraries on 1.8%

agarose gels and extracted a 400 bp band. The bands were purified (Macherey-Nagel Nucleospic Gel and PCR Cleanup kit) and bioanalyzed as a final quality control check. Each library was submitted to the UC Davis DNA Technologies core for 250 x 250 paired end, dual index sequencing on an Illumina MiSeq instrument.

Sequence Analysis

The sequences obtained from the MiSeq runs were demultiplexed based on the barcode sequences using a custom Perl script based upon exact matching. The sequences were overlapped to form contiguous reads using MOTHUR's command make.contigs (5). Reads containing any ambiguous bases were then discarded along with any reads that were over 275 bp. The sequences were then clustered into operational taxonomic units (OTUs) by UCLUST (6) based on 97% pairwise identity using QIIME's (7) open reference OTU picking strategy which used the Greengenes 16S rRNA database (13_5 release) as a reference (8). Taxonomic classification of the representative sequence for each OTU was done using QIIME's version of the Ribosomal Database Project's classifier (9) against the Greengenes 16S rRNA database (13_5 release) using default parameters. All OTUs identified as belonging to chloroplast and mitochondria were removed from the data set. The representative sequences for each OTU were aligned using PyNAST (10) in QIIME. Chimeric OTUs were identified using QIIME's implementation of ChimeraSlayer (11) and removed from the OTU table and OTU representative sequences file. A phylogenetic tree was generated from the alignment file by FastTree (12).

Statistical Analysis

The resulting OTU table was divided by experiment and analyzed separately except when comparing methanogenic and methanotrophic OTUs. Low abundance OTUs were eliminated from the OTU table if they did not have a total of at least 5 counts across all the samples in the experiment.. OTU tables for each experiment were normalized by the trimmed mean of M values (TMM) method using the BioConductor package EdgeR in R (13). Weighted and Unweighted UniFrac (14) distances were calculated from the normalized OTU tables for each experiment. α-diversity measurements were calculated by the function diversity() using the "Shannon" method in the R package Vegan (15).

129 Rarefaction curves were calculated using custom R scripts. Principal coordinate analyses utilizing the
130 weighted and unweighted UniFrac distances were calculated using the pcoa() function from the R
131 package Ape (16). CAP analysis was performed using the function capscale() from the R Package Vegan.
132 When specifying CAP models, we constrained the analysis to the factor of interest while controlling for
133 all other experimental factors and technical factors (MiSeq runs). Variance partitioning and significances
134 for experimental factors was performed by running Vegan's permutest() function over the CAP model
135 using a maximum of 500 permutations. Bulk soil samples were omitted from the CAP analysis when
136 analyzing the greenhouse data. This was done because the bulk soil samples provided a confounding
137 level within the *Cultivar* factor. Additionally, permutational MANOVA was carried out to using Vegan's
138 function adonis() to measure effect size and significances on β-diversity. Differentially abundant OTUs
139 were detected using EdgeR's generalized linear model (GLM) approach. This approach allows the user to
140 test for differential OTU abundance between different levels of factors by employing a design matrix to
141 account for complex experimental designs.

142 **Co-abundance network analysis**

143 Only OTUs that were determined to be differentially abundant in experimental factors
144 encompassed in the field experiment were used for network analysis, thus subsetting the data to OTUs
145 with high variance (10,848 OTUs). Pairwise Pearson correlations were calculated between the remaining
146 OTUs. The Pearson correlations were used as a distance metric to build a hierarchically clustered
147 dendrogram using average linkage. The dendrogram was dynamically pruned using the R package
148 'dynamicTreeCut' (17). This tree cutting technique was employed due to its ability to detect nested
149 clusters within larger clusters. A hypergeometric test was used to detect taxonomies that were
150 significantly enriched in specific clusters. Taxonomies were queried for their involvement in methane
151 metabolism and cycling using the BioCyc (18), MetaCyc (18), or KEGG Pathway (19) databases unless
152 otherwise noted.

153 **CARD-FISH**

154 Roots designated for CARD-FISH were fixed using 4% formaldehyde in PBS for 4 hours,

washed twice with PBS, and stored in 1:1 ethanol:PBS at 4° C. CARD-FISH treatments were done in accordance with previous studies in *Arabidopsis* (2, 3, 20) using the eubacterial probe Eub338 (5'-GCTGCCTCCCGTAGGAGT-3', 35% formamide, Biomers Ulm, Germany) and its nonsense sequence as a negative control, NON338 (5'- ACTCCTACGGGAGGCAGC-3', 30% formamide) labeled with horseradish peroxidase at the 5' end (Biomers Ulm, Germany). Signal amplification was carried out using fluorescently labeled tyramide (Fluorescent solutions). All microscopy images were taken using a confocal laser scanning microscope in the Department of Plant Biology at UC Davis (Zeiss LSM 710).

Amplification, cloning, and sequencing of *mcrA*.

Total community DNA extracted from rhizosphere and endosphere samples from the DS RR field was used as a template to amplify fragments of the *mcrA* gene. PCR was performed following the protocol described in Juottonen et al. (21) using the primers designed in Springer et al. (22) The amplified products were cloned with the TOPO TA cloning kit (Invitrogen), and plasmid DNA was recovered from 47 clones (29 from endosphere samples and 18 from rhizosphere samples) using GeneJET plasmid miniprep kit (Thermo Scientific). The cloned fragments were sequenced by the UC Davis Sequencing Facility using the M13 primers. A BLAST search was performed using the NCBI nucleotide database, and the top alignment was reported for each sequence (alignments without a defined taxonomy were excluded).

References

1. Bulgarelli D, Schlaeppi K, Spaepen S, van Themaat EVL, & Schulze-Lefert P (2013) Structure and functions of the bacterial microbiota of plants. *Annual review of plant biology* 64:807-838.
2. Bulgarelli D*, et al.* (2012) Revealing structure and assembly cues for Arabidopsis root-inhabiting bacterial microbiota. *Nature* 488(7409):91-95.
3. Lundberg DS*, et al.* (2012) Defining the core Arabidopsis thaliana root microbiome. *Nature* 488(7409):86-90.
4. Caporaso JG*, et al.* (2011) Global patterns of 16S rRNA diversity at a depth of millions of sequences per sample. *Proceedings of the National Academy of Sciences* 108(Supplement 1):4516-4522.
5. Schloss PD*, et al.* (2009) Introducing mothur: open-source, platform-independent, community-supported software for describing and comparing microbial communities. *Applied and environmental microbiology* 75(23):7537-7541.

6. Edgar RC (2010) Search and clustering orders of magnitude faster than BLAST. *Bioinformatics* 26(19):2460-2461.
7. Caporaso JG*, et al.* (2010) QIIME allows analysis of high-throughput community sequencing data. *Nature methods* 7(5):335-336.
8. DeSantis TZ*, et al.* (2006) Greengenes, a chimera-checked 16S rRNA gene database and workbench compatible with ARB. *Applied and environmental microbiology* 72(7):5069-5072.
9. Cole JR*, et al.* (2009) The Ribosomal Database Project: improved alignments and new tools for rRNA analysis. *Nucleic acids research* 37(suppl 1):D141-D145.
10. Caporaso JG*, et al.* (2010) PyNAST: a flexible tool for aligning sequences to a template alignment. *Bioinformatics* 26(2):266-267.
11. Haas BJ*, et al.* (2011) Chimeric 16S rRNA sequence formation and detection in Sanger and 454-pyrosequenced PCR amplicons. *Genome research* 21(3):494-504.
12. Price MN, Dehal PS, & Arkin AP (2009) FastTree: computing large minimum evolution trees with profiles instead of a distance matrix. *Molecular biology and evolution* 26(7):1641-1650.
13. Robinson MD, McCarthy DJ, & Smyth GK (2010) edgeR: a Bioconductor package for differential expression analysis of digital gene expression data. *Bioinformatics* 26(1):139-11.
14. Lozupone C & Knight R (2005) UniFrac: a new phylogenetic method for comparing microbial communities. *Applied and environmental microbiology* 71(12):8228-8235.
15. Oksanen J*, et al.* (2007) The vegan package. *Community ecology package*.
16. Paradis E, Claude J, & Strimmer K (2004) APE: analyses of phylogenetics and evolution in R language. *Bioinformatics* 20(2):289-290.
17. Langfelder P, Zhang B, & Horvath S (2008) Defining clusters from a hierarchical cluster tree: the Dynamic Tree Cut package for R. *Bioinformatics* 24(5):719-720.
18. Caspi R*, et al.* (2008) The MetaCyc Database of metabolic pathways and enzymes and the BioCyc collection of Pathway/Genome Databases. *Nucleic acids research* 36(suppl 1):D623-D631.
19. Kanehisa M & Goto S (2000) KEGG: kyoto encyclopedia of genes and genomes. *Nucleic acids research* 28(1):27-30.
20. Eickhorst T & Tippkötter R (2008) Improved detection of soil microorganisms using fluorescence *in situ* hybridization (FISH) and catalyzed reporter deposition (CARD-FISH). *Soil Biology and Biochemistry* 40(7):1883-1891.
21. Juottonen H, Galand PE, & Yrjälä K (2006) Detection of methanogenic Archaea in peat: comparison of PCR primers targeting the *mcrA* gene. *Research in microbiology* 157(10):914-921.
22. Springer E, Sachs MS, Woese CR, & Boone DR (1995) Partial gene sequences for the A subunit of methyl-coenzyme M reductase (mcrI) as a phylogenetic tool for the family Methanosarcinaceae. *International Journal of Systematic Bacteriology* 45(3):554-559.

Supplementary Figures

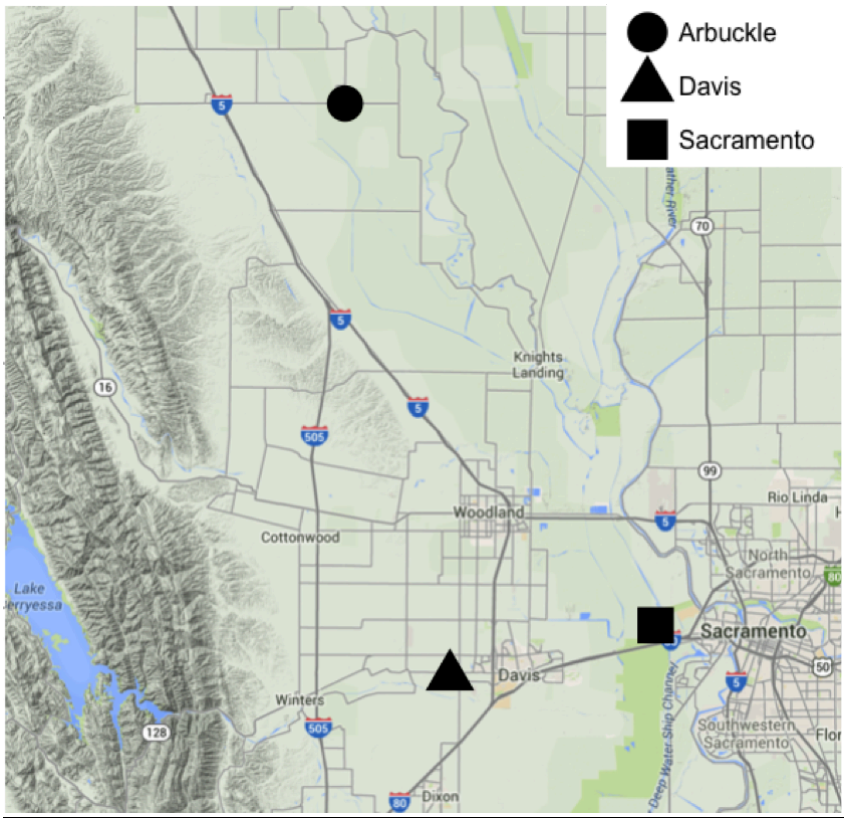

Fig. S1 Map depicting soil collection locations for greenhouse experiment.

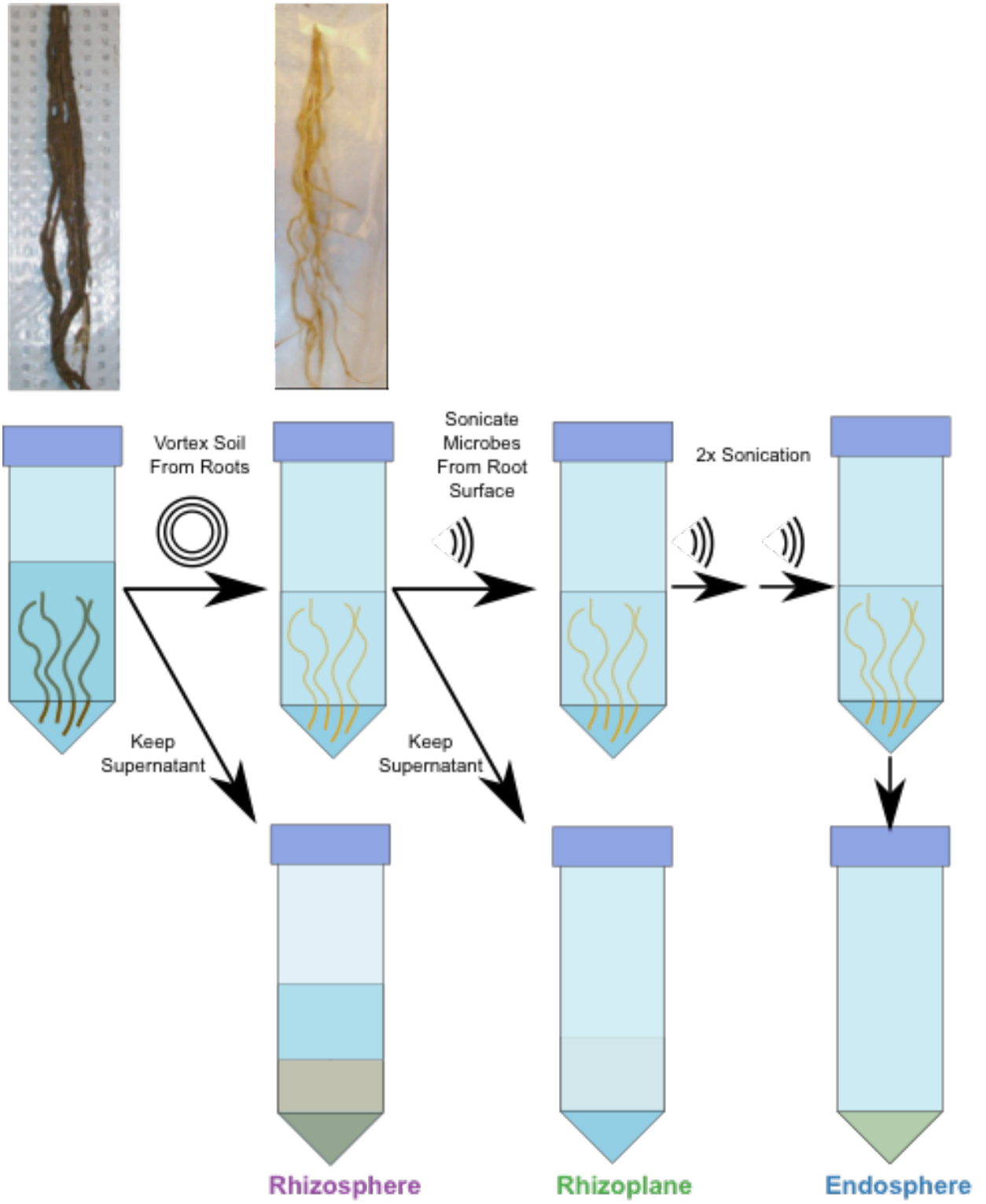

234

235 **Fig. S2. Sampling and collection of the rhizocompartments.** Roots are collected from rice

236 plants and soil is shaken off the roots to leave ~1mm of soil around the roots. The ~1 mm of soil

is washed off in PBS and kept as the rhizosphere compartment. The clean roots are then washed twice more to remove remaining soil and placed into clean PBS in a 50 mL Falcon tube. The rhizoplane microbes are extracted by sonicating the roots with the rhizosphere compartment removed. The sonicated roots are then placed in a new, clean Falcon tube and sonicated twice more, decanting the PBS in the tube between sonications and refilling with clean PBS. These roots are then kept for extracting the endospheric microbes.

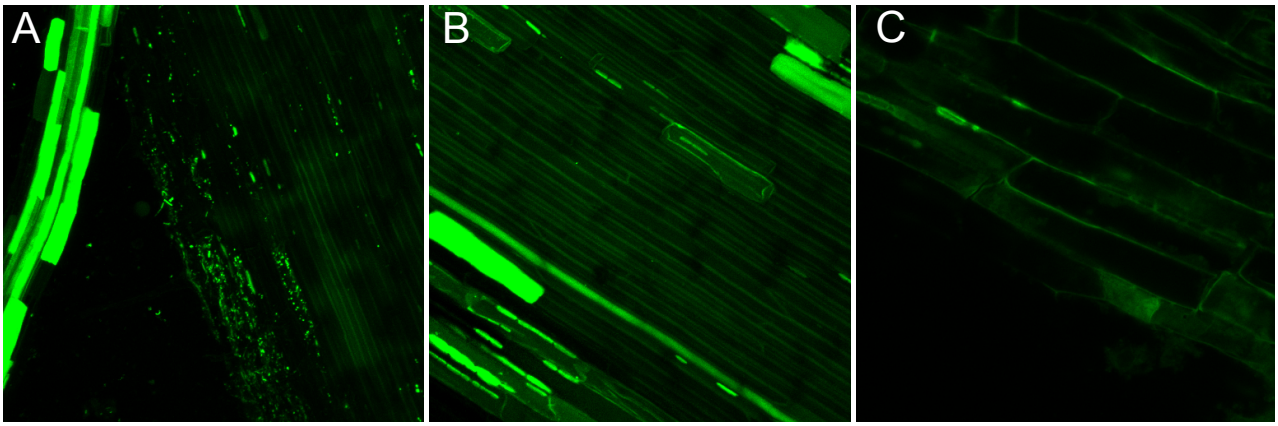

Fig. S3. CARD-FISH reveals that rhizoplane microbes are removed after sonication of rice roots. (**A**) Pre-sonicated root incubated with the Eub338 eubacterial probe. (B) Thrice sonicated root incubated with the Eub338 eubacterial probe. (C) Pre-sonicated root probed with the antisense Eub338 probe as a negative control. Files of root cells showing bright signals are presumed to be dead cells damaged during the removal of rhizosphere soil.

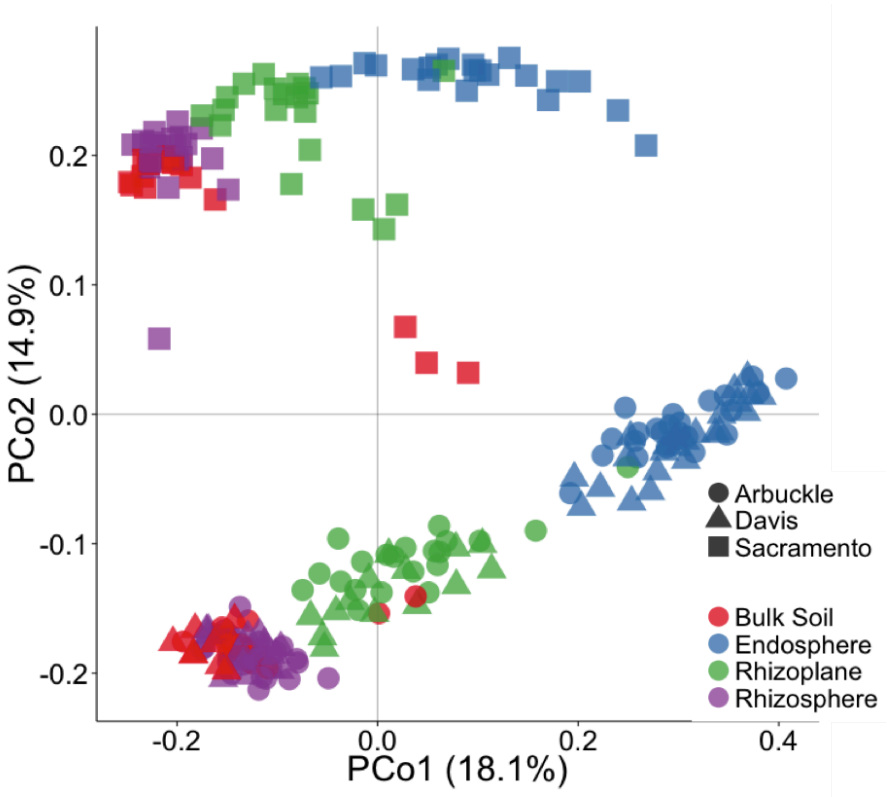

277

278 **Fig. S4. Rice root-associated microbiomes vary by rhizocompartment and site in the**

279 **greenhouse experiment.** PCoA using the unweighted UniFrac distance metric indicates that

280 microbiomes separate by rhizocompartment and soil source.

281

282

283

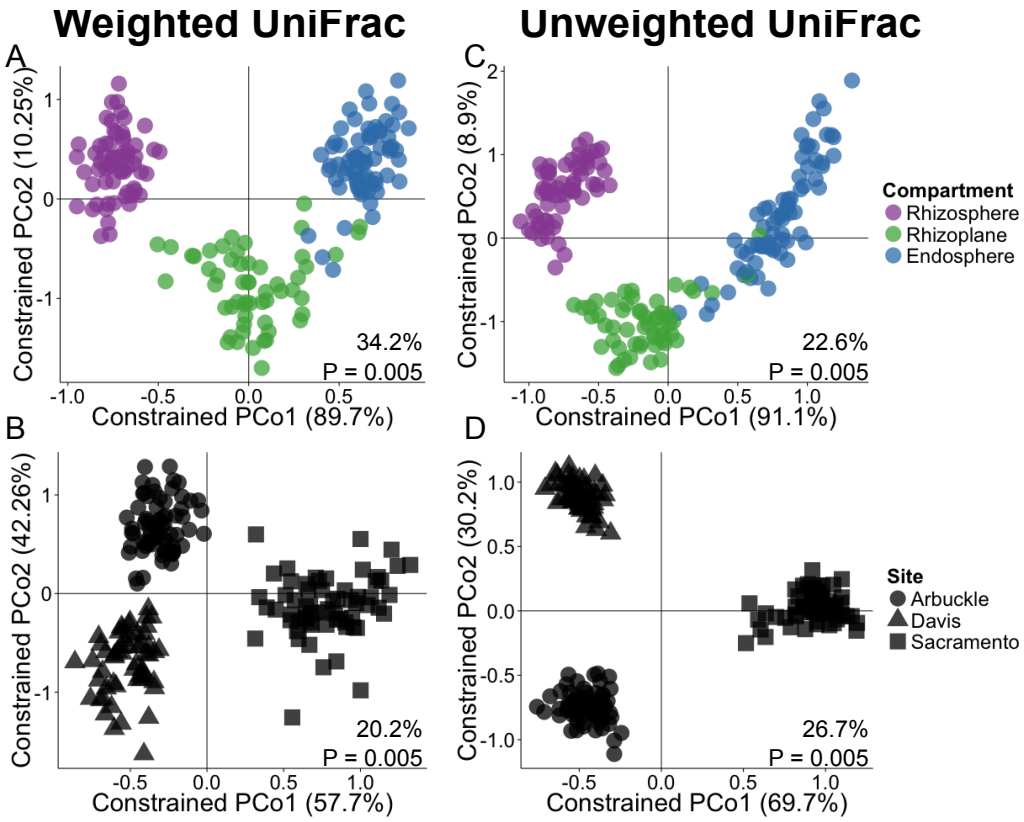

284

285 **Fig. S5. CAP analysis confirms that rice root microbiomes vary by compartment and soil**
286 **source.** (**A**) CAP analysis ordination constrained to rhizocompartment and conditioned on soil
287 source, cultivar, and technical factors using the weighted UniFrac distance metric. (**B**) CAP
288 analysis ordination constrained to soil source and conditioned on rhizocompartment, cultivar,
289 and technical factors using the weighted UniFrac distance metric. (**C**) CAP analysis ordination
290 constrained to rhizocompartment and conditioned on soil source, cultivar, and technical factors
291 using the unweighted UniFrac distance metric. (**D**) CAP analysis ordination constrained to soil
292 source and conditioned on rhizocompartment, cultivar, and technical factors using the weighted
293 UniFrac distance metric. All variances attributable to the constrained factor and the significance
294 of the factor are portrayed in each plot.

295

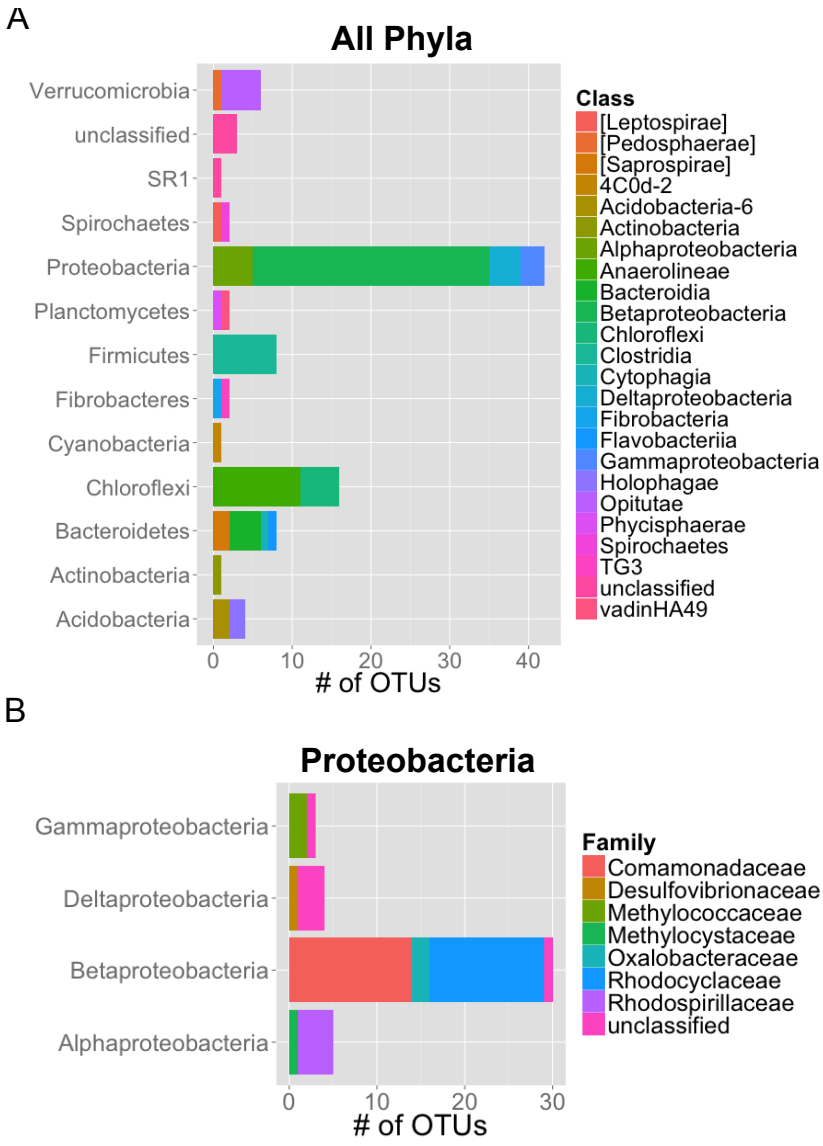

Fig. S6. A set of 96 OTUs mainly consisting of Proteobacteria is enriched across every compartment in the greenhouse experiment. (**A**) Number of OTUs and the phyla and classes they belong to that are enriched across all rhizocompartments in the greenhouse experiment. (**B**) A subset of the Proteobacteria and the classes and families they belong to in the OTUs that are enriched across all rhizocompartments in the greenhouse.

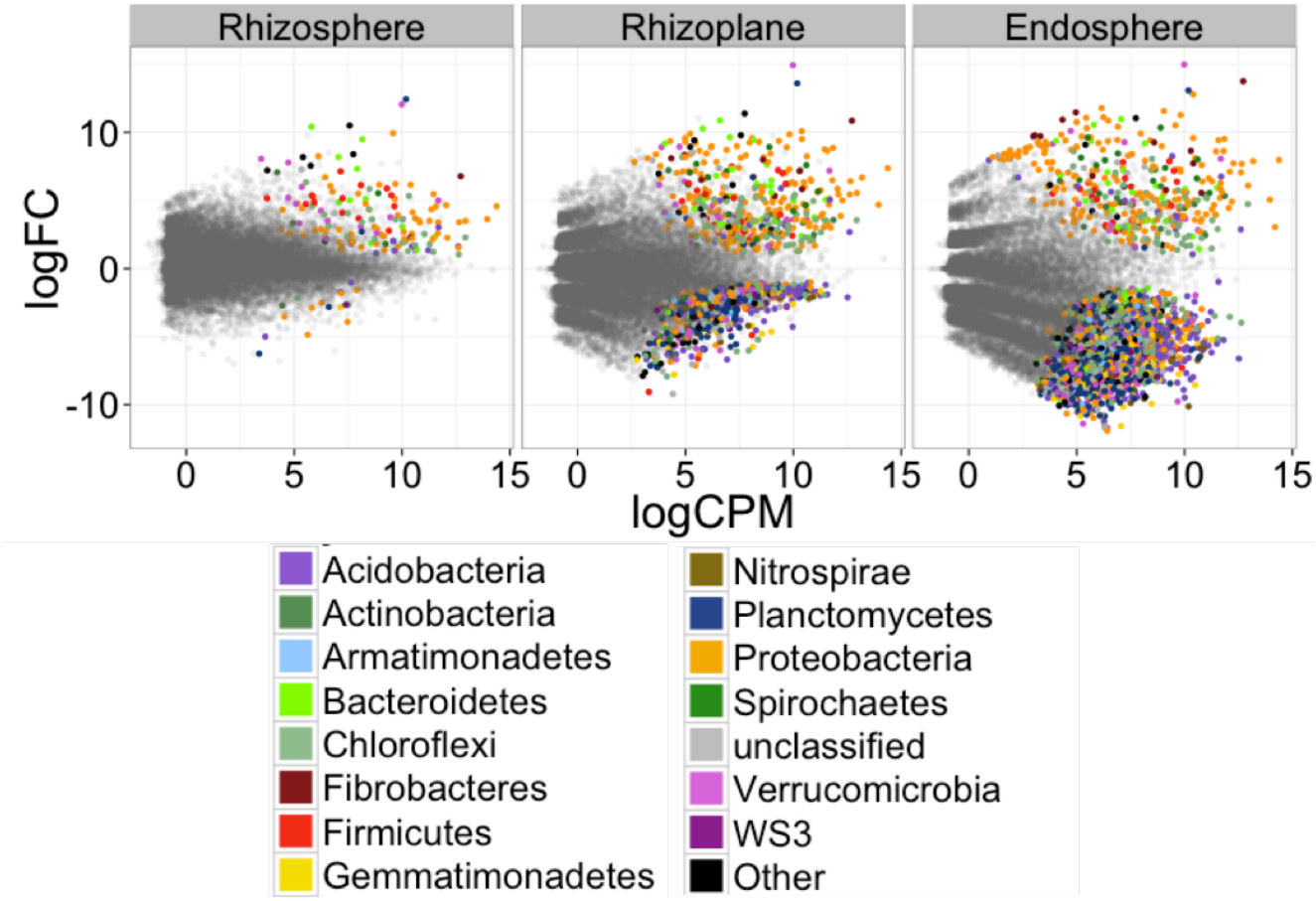

Fig. S7 Microbes enriched and depleted in the rhizocompartments compared to bulk soil have taxonomic patterns. Each point represents one OTU and the color of the point represents the OTU's assigned Phyla.

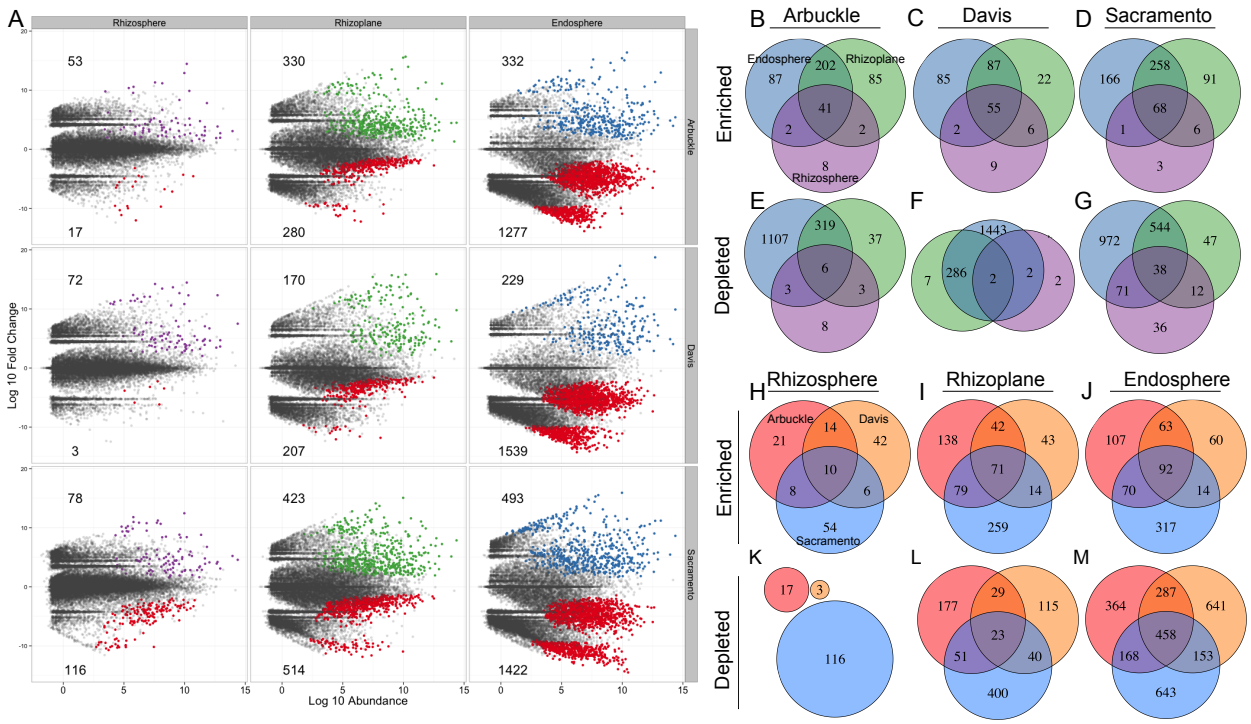

Fig. S8. The different soil sources have commonalities and differences in differentially abundant OTUs. (**a**) MVA plots representing enrichment and depletion of OTUs in each compartment compared to bulk soil across each soil source in the greenhouse experiment. (**b**) A venn diagram comparing differentially enriched OTUs in each compartment in Arbuckle soil. (**c**) A venn diagram comparing differentially enriched OTUs in each compartment in Davis soil. (**d**) A venn diagram comparing differentially enriched OTUs in each compartment in Sacramento soil. (**e**) A venn diagram comparing differentially depleted OTUs in each compartment in Arbuckle soil. (**f**) A venn diagram comparing differentially depleted OTUs in each compartment in Davis soil. (**g**) A venn diagram comparing differentially depleted OTUs in each compartment in Sacramento soil. (**h**) A venn diagram comparing differentially enriched OTUs in each soil for the rhizosphere compartment. (**i**) A venn diagram comparing differentially enriched OTUs in each soil for the rhizoplane compartment. (**j**) A venn diagram comparing differentially enriched OTUs in each soil for the endosphere compartment. (**k**) A venn diagram comparing differentially

depleted OTUs in each soil for the rhizosphere compartment. (**l**) A venn diagram comparing differentially depleted OTUs in each soil for the rhizoplane compartment. (**m**) A venn diagram comparing differentially depleted OTUs in each soil for the endosphere compartment. Coloration is consistent for rhizocompartments across (b) to (g) and consistent for soil sources across (h) to (m).

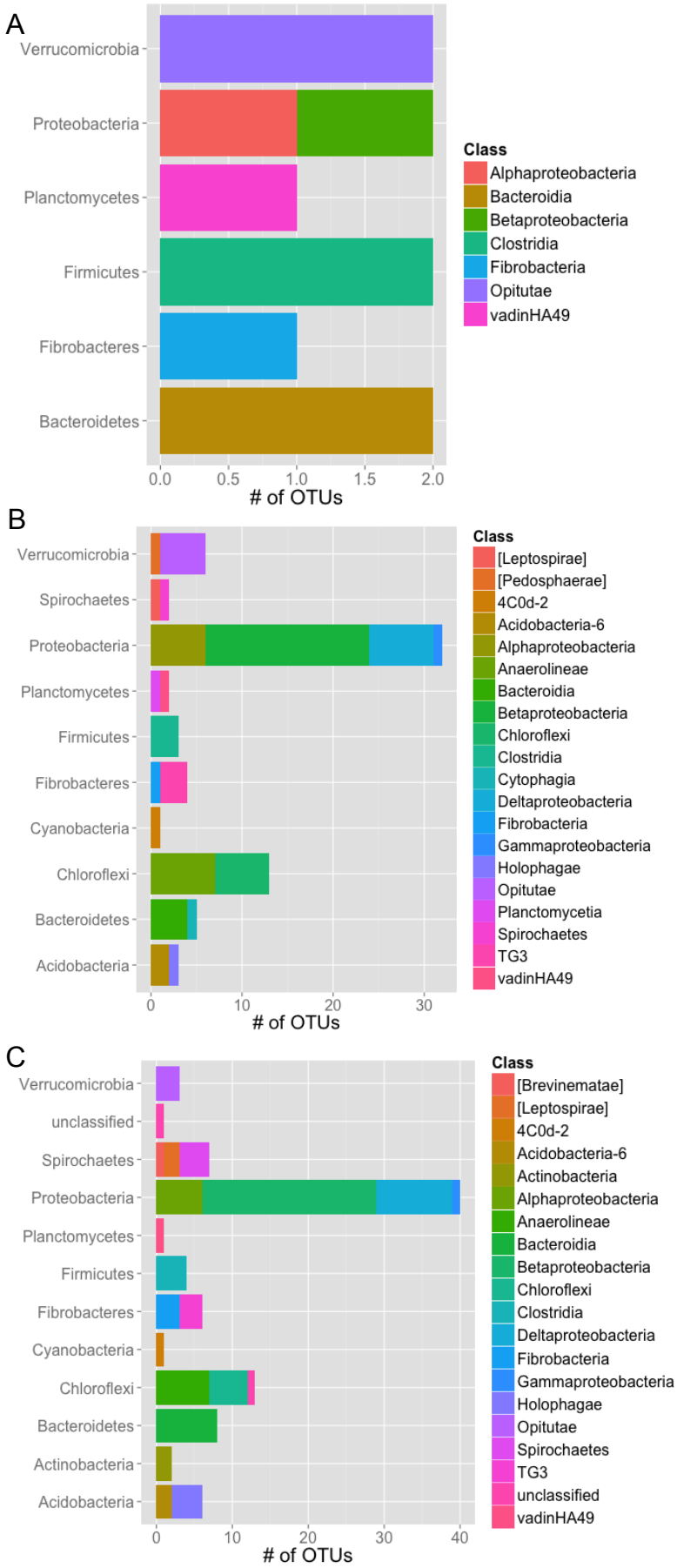
A
Verrucomicrobia
Proteobacteria
Planctomycetes
Firmicutes
Fibrobacteres
Bacteroidetes
0.0
0.5
1.0
1.5
2.0
# of OTUs
Class
Alphaproteobacteria
Bacteroidia
Betaproteobacteria
Clostridia
Fibrobacteria
Opitutae
vadinHA49
B
Verrucomicrobia
Spirochaetes
Proteobacteria
Planctomycetes
Firmicutes
Fibrobacteres
Cyanobacteria
Chloroflexi
Bacteroidetes
Acidobacteria
0
10
20
30
# of OTUs
Class
[Leptospirae]
[Pedosphaerae]
4C0d-2
Acidobacteria-6
Alphaproteobacteria
Anaerolineae
Bacteroidia
Betaproteobacteria
Chloroflexi
Clostridia
Cytophagia
Deltaproteobacteria
Fibrobacteria
Gammaproteobacteria
Holophagae
Opitutae
Planctomycetia
Spirochaetes
TG3
vadinHA49
C
Verrucomicrobia
unclassified
Spirochaetes
Proteobacteria
Planctomycetes
Firmicutes
Fibrobacteres
Cyanobacteria
Chloroflexi
Bacteroidetes
Actinobacteria
Acidobacteria
0
10
20
30
40
# of OTUs
Class
[Brevinematae]
[Leptospirae]
4C0d-2
Acidobacteria-6
Actinobacteria
Alphaproteobacteria
Anaerolineae
Bacteroidia
Betaproteobacteria
Chloroflexi
Clostridia
Deltaproteobacteria
Fibrobacteria
Gammaproteobacteria
Holophagae
Opitutae
Spirochaetes
TG3
unclassified
vadinHA49

Fig. S9. Rice plants grown in diverse soil sources have commonalities in enriched OTUs in each rhizocompartment. Plants grown in Davis, Arbuckle, and Sacramento soil share enriched OTUs in the (**A**) rhizosphere, (**B**) rhizoplane, and (**C**) endosphere.

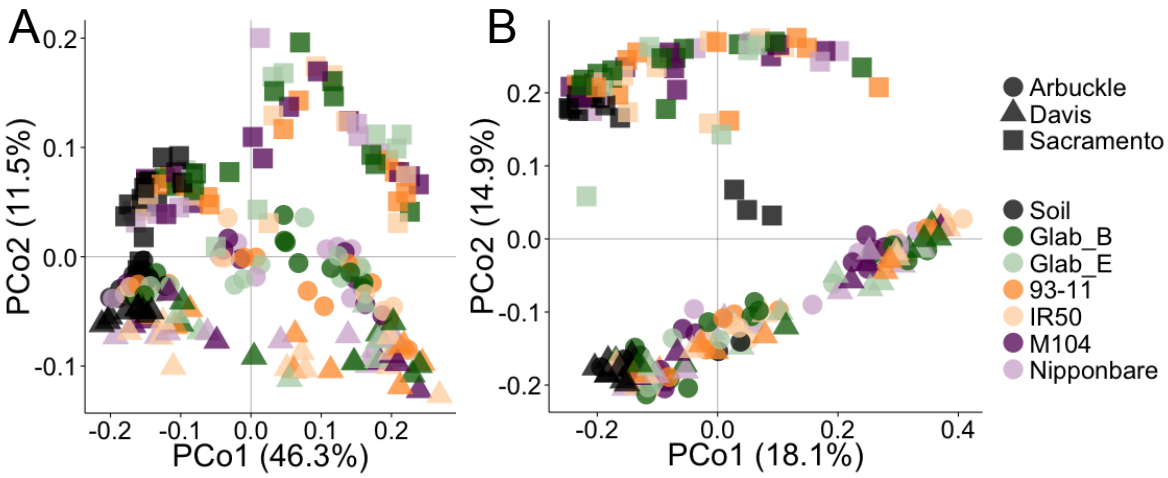

Fig S10. Unconstrained PCoA reveals no distinct clustering of microbiomes of different rice cultivars. (**A**) Unconstrained PCoA using the weighted UniFrac distance metric. (**B**) Unconstrained PCoA using the unweighted UniFrac distance metric.

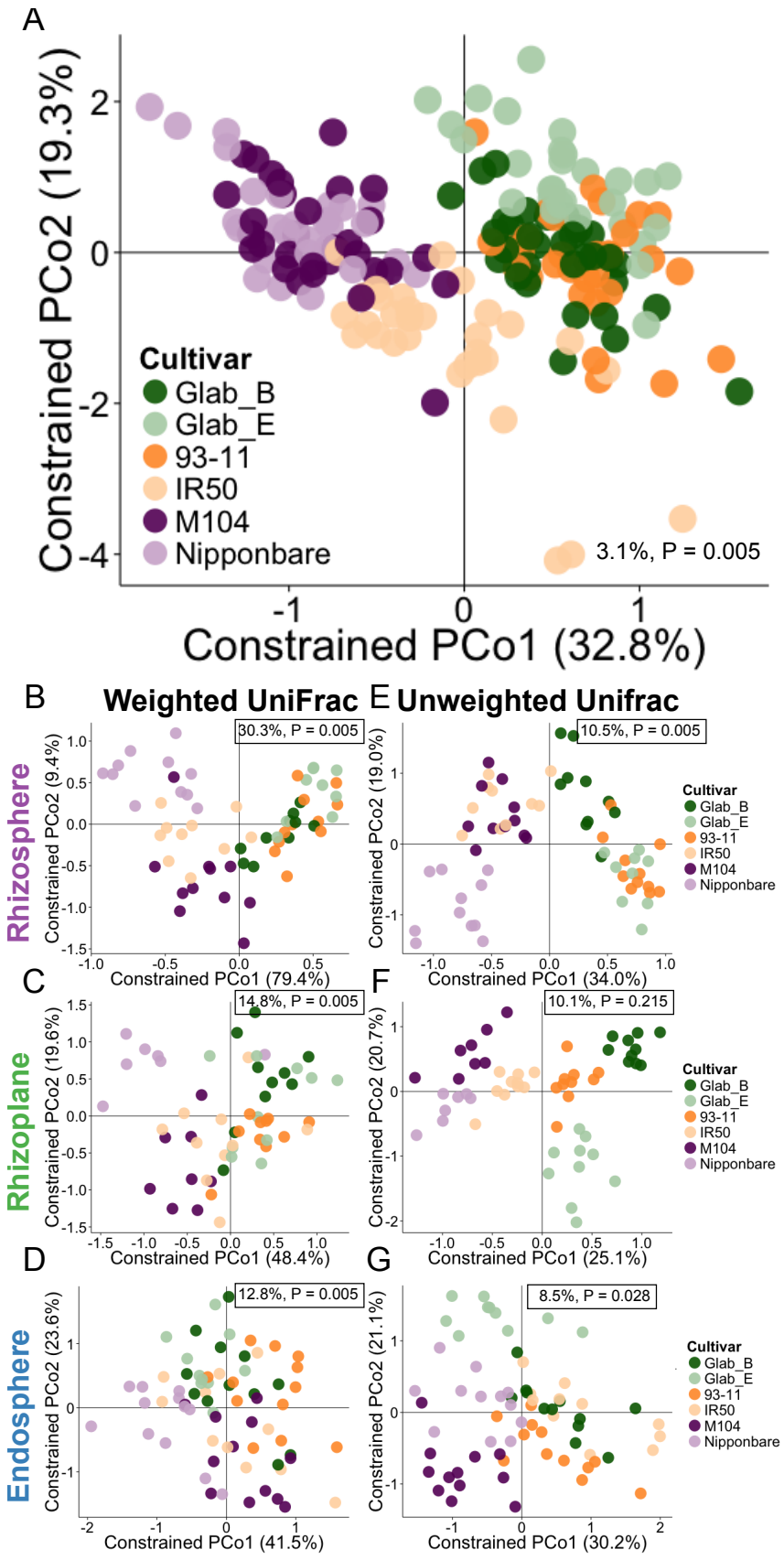
A
Constrained PCo2 (19.3%)
Constrained PCo1 (32.8%)
Cultivar
Glab_B
Glab_E
93-11
IR50
M104
Nipponbare
3.1%, P = 0.005
B
Weighted UniFrac
E
Unweighted Unifrac
Rhizosphere
30.3%, P = 0.005
Constrained PCo2 (9.4%)
Constrained PCo1 (79.4%)
10.5%, P = 0.005
Constrained PCo2 (19.0%)
Constrained PCo1 (34.0%)
C
F
Rhizoplane
14.8%, P = 0.005
Constrained PCo2 (19.6%)
Constrained PCo1 (48.4%)
10.1%, P = 0.215
Constrained PCo2 (20.7%)
Constrained PCo1 (25.1%)
D
G
Endosphere
12.8%, P = 0.005
Constrained PCo2 (23.6%)
Constrained PCo1 (41.5%)
8.5%, P = 0.028
Constrained PCo2 (21.1%)
Constrained PCo1 (30.2%)

393

Fig S11. CAP analysis constrained to rice cultivar while conditioning on rhizocompartment, soil source, and technical factors reveals distinct clustering patterns of microbiomes between rice genotypes. (**A**) CAP analysis of the whole data using the unweighted UniFrac distance metric. (**B - D**) CAP analysis constrained to rice cultivar using the weighted UniFrac distance metric for (**B**) the rhizosphere samples, (**C**) the rhizoplane samples, (**D**) the endosphere samples. (**E – G**) CAP analysis constrained to rice cultivar using the unweighted distance metric for (**E**) the rhizosphere samples, (**F**) the rhizoplane samples, (**G**) the endosphere samples. All variances attributable to the constrained factor and the significance of the factor are portrayed in each plot.

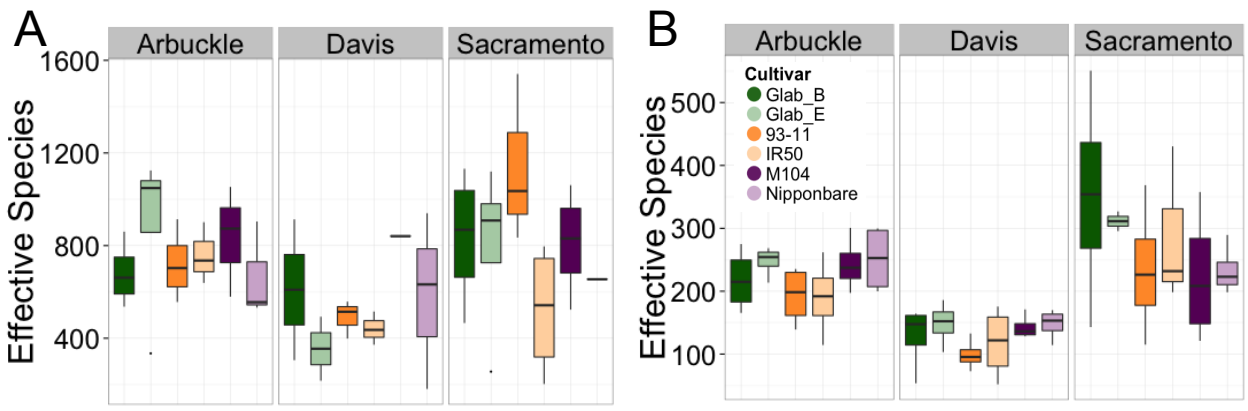

Fig S12. Alpha diversities microbes on the rhizoplane and endosphere of rice cultivars grown in different show no genotypic patterns. (**A**) Rhizoplane alpha diversities. (**B**) Endosphere alpha diversities.

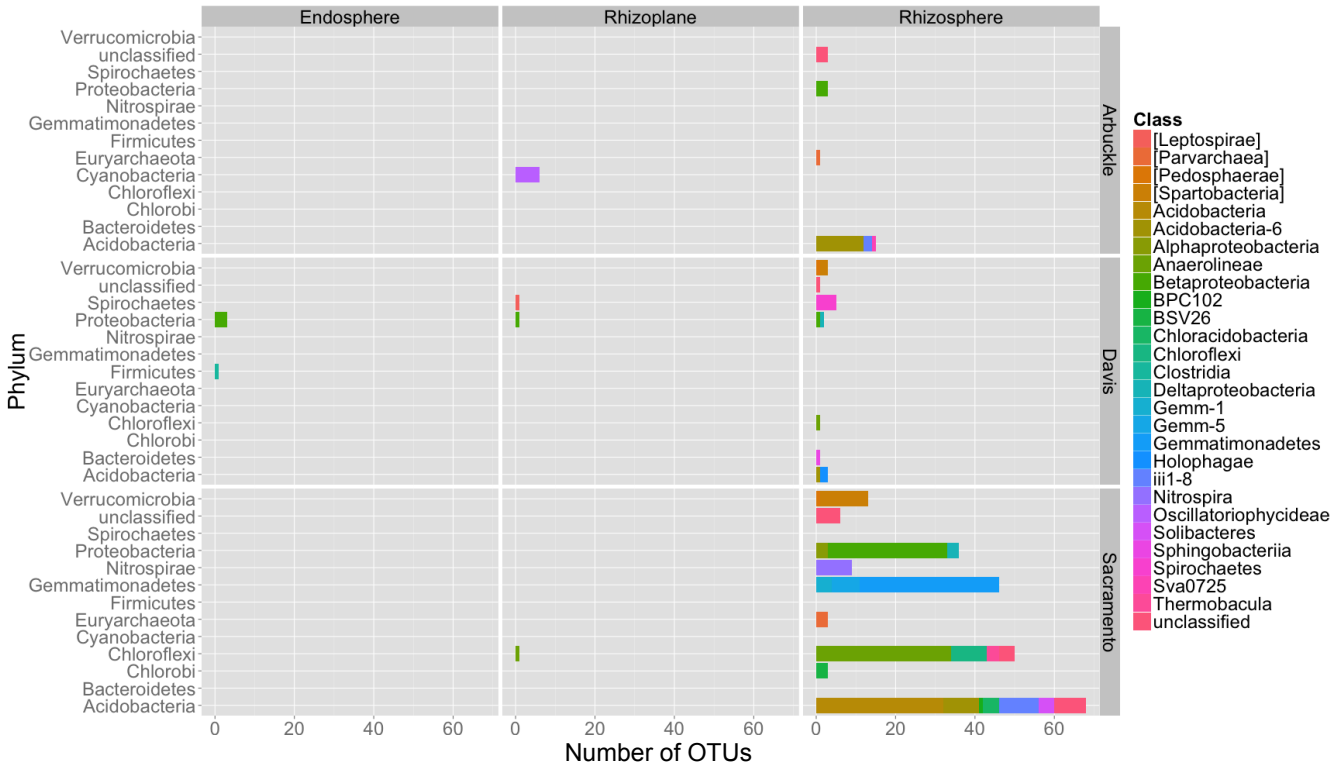

Fig. S13. Differentially abundant OTUs between rice cultivars in each rhizocompartment and soil source.

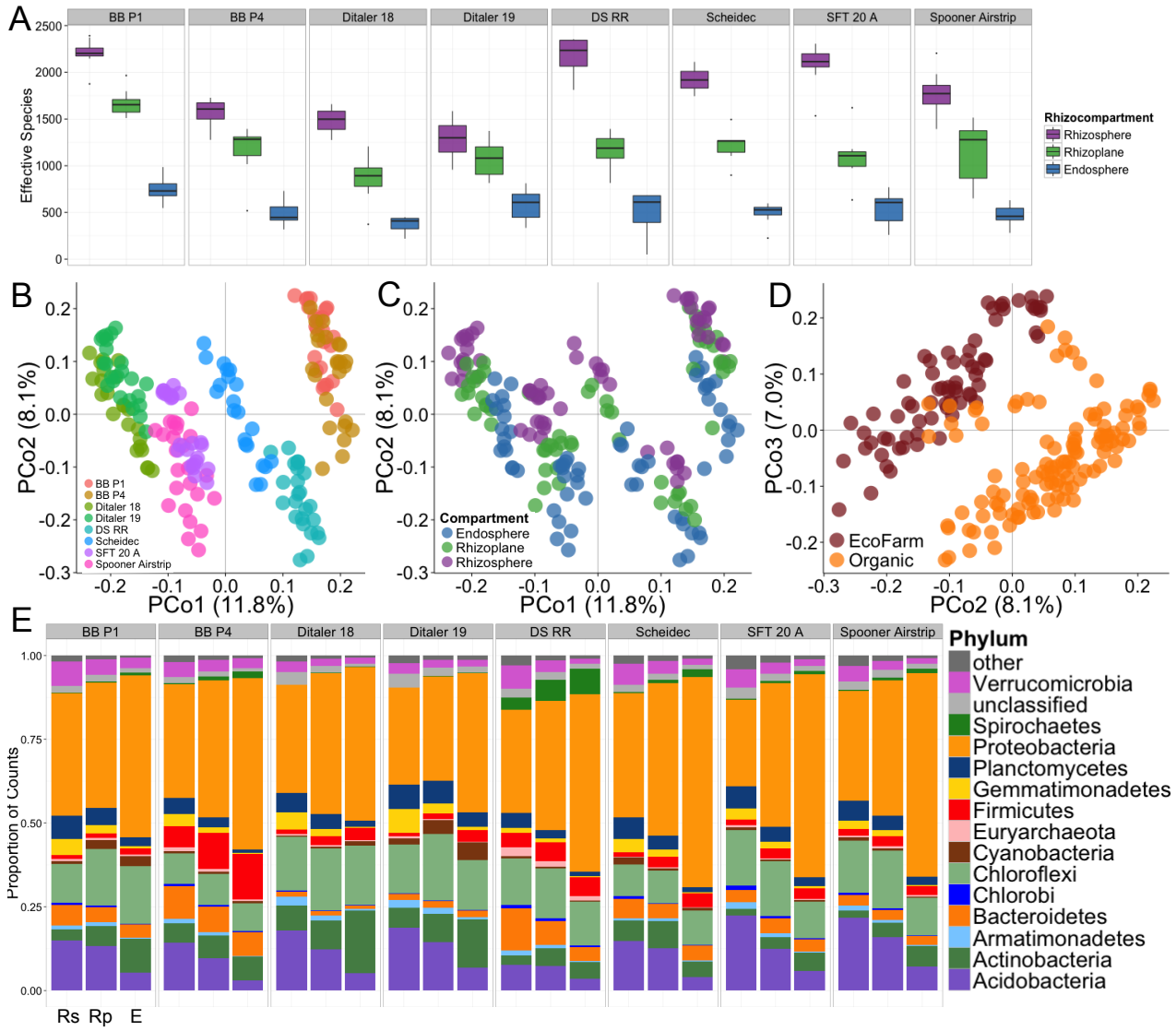

Fig. S14. A gradient of diversity exists in the rhizocompartments of field grown rice. (**a**) α-diversity (Shannon) of all rhizocompartments sampled from all fields. (**b**) PCoA using the weighted UniFrac metric colored by field site. (**c**) Same PCoA and axes as represented in (b), colored by rhizocompartment. (**d**) Same PCoA represented in (b) and (c), axes 2 and 3 are shown and colored by cultivation practice. (**e**) Distribution of phyla across each rhizocompartment and every field. Rs, Rhizosphere; Rp Rhizoplane; E, Endosphere.

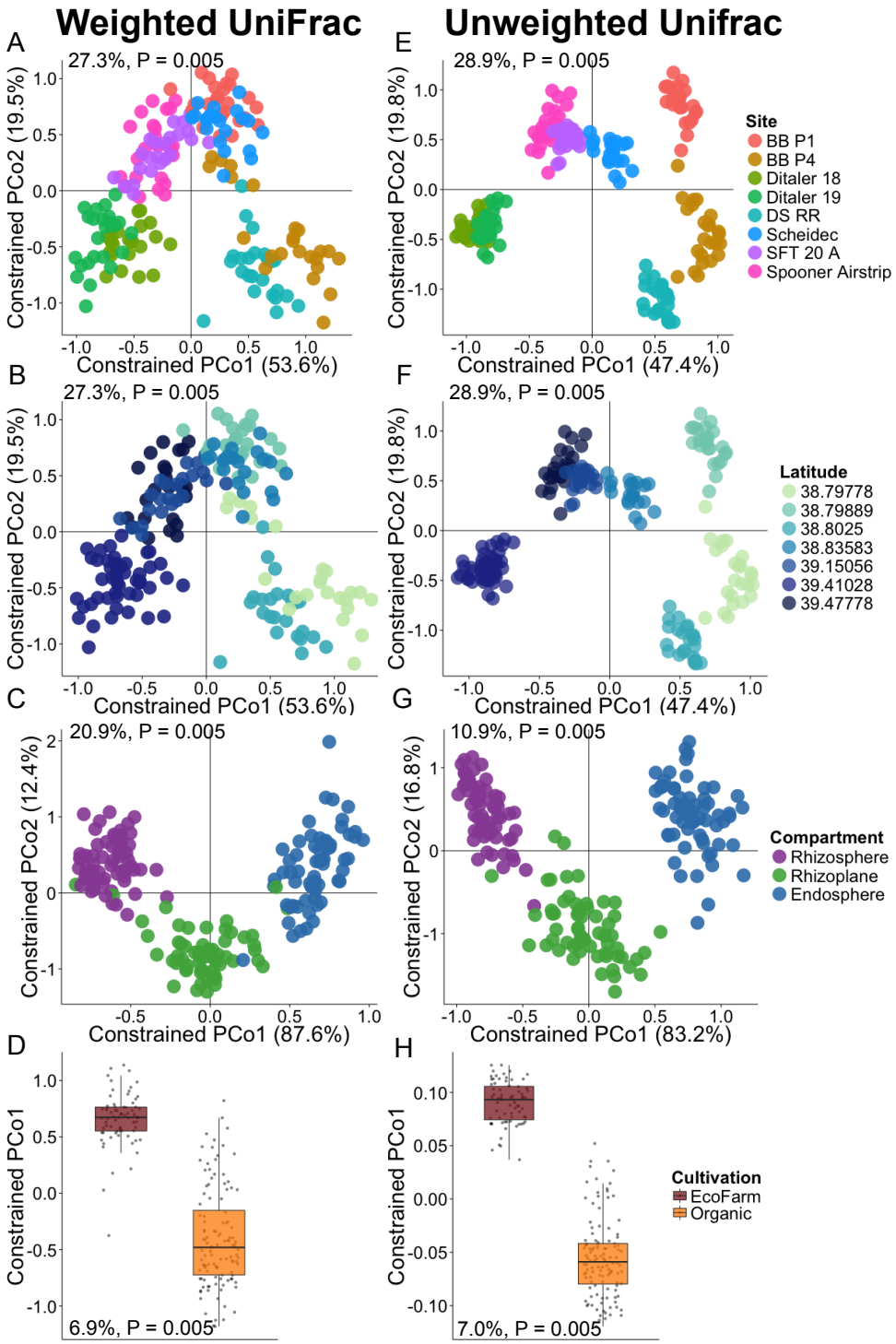

458

459 **Fig. S15. CAP analysis of the field data reveals that microbiomes vary by**

460 **rhizocompartment, field site, and cultivation practice.** (**A – D**) CAP analysis using the

461 weighted UniFrac metric. (**A**) CAP analysis constrained to field site and conditioning on

rhizocompartment, cultivation practice, and technical factors. (**B**) Same analysis as (**A**) but colored by latitude. (**C**) CAP analysis constrained to rhizocompartment conditioned on field site, cultivation practice, and technical factors. (**D**) CAP analysis on constrained to cultivation practice. (**E – H**) CAP analysis using the unweighted UniFrac metric. (**E**) CAP analysis constrained to field site and conditioning on rhizocompartment, cultivation practice, and technical factors. (**F**) Same analysis as (**E**) but colored by latitude. (**G**) CAP analysis constrained to rhizocompartment conditioned on field site, cultivation practice, and technical factors. (**H**) CAP analysis on constrained to cultivation practice. All variances attributable to the constrained factor and the significance of the factor are portrayed in each plot.

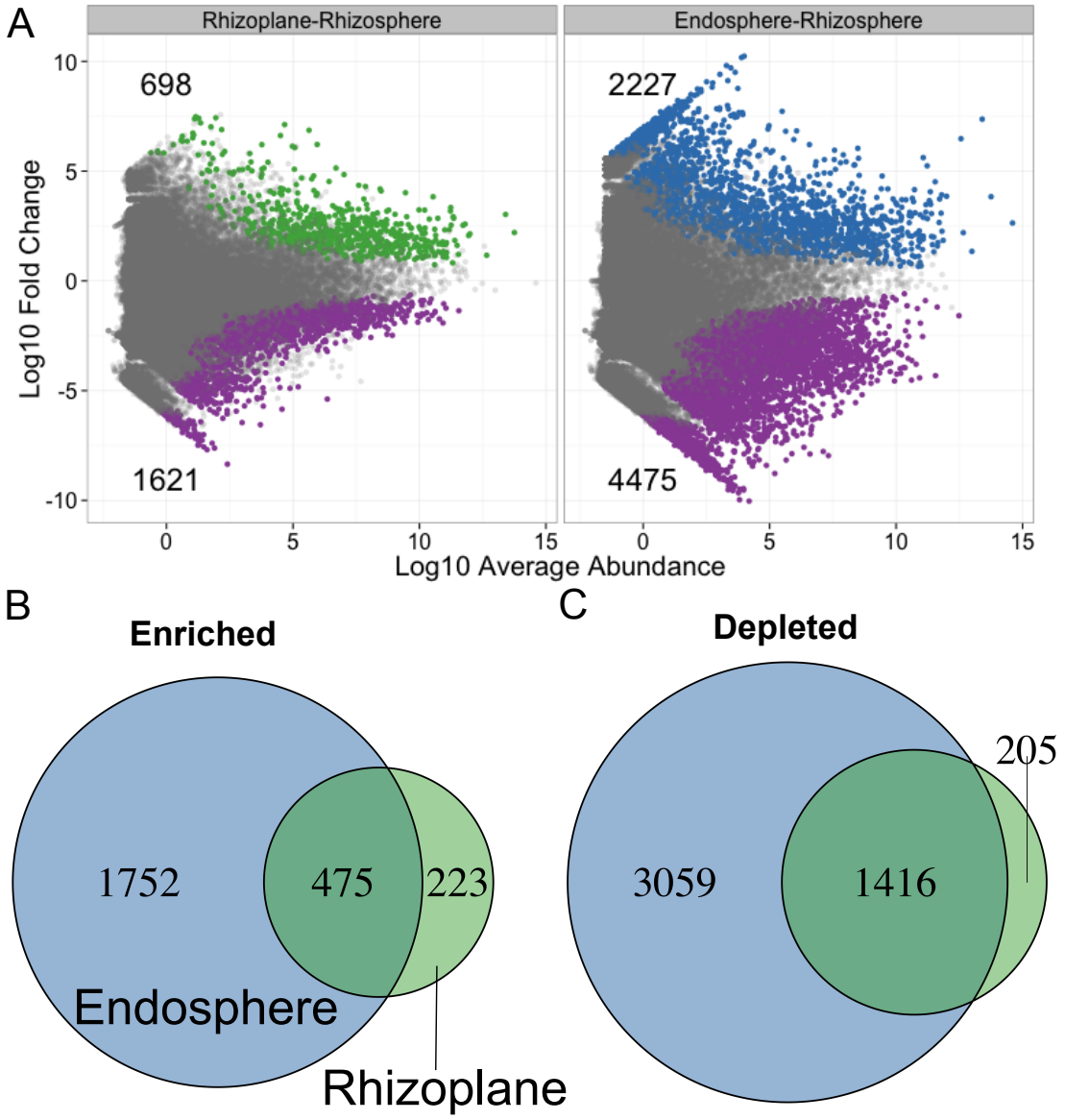

485

486 **Fig. S16. The rhizocompartments of field grown plants are enriched and depleted for**

487 **OTUs.** (**a**) MVA plot displaying enriched OTUs in the endosphere and the rhizoplane compared

488 to the rhizosphere. (**b**) Venn diagram displaying similarities and differences among significantly

489 enriched OTUs in the rhizoplane and endosphere. (**c**) Venn diagram displaying the similarities

490 and differences among significantly depleted OTUs in the rhizoplane and endosphere. The color

491 scheme is consistent of the rhizocompartments in the venn diagrams.

492

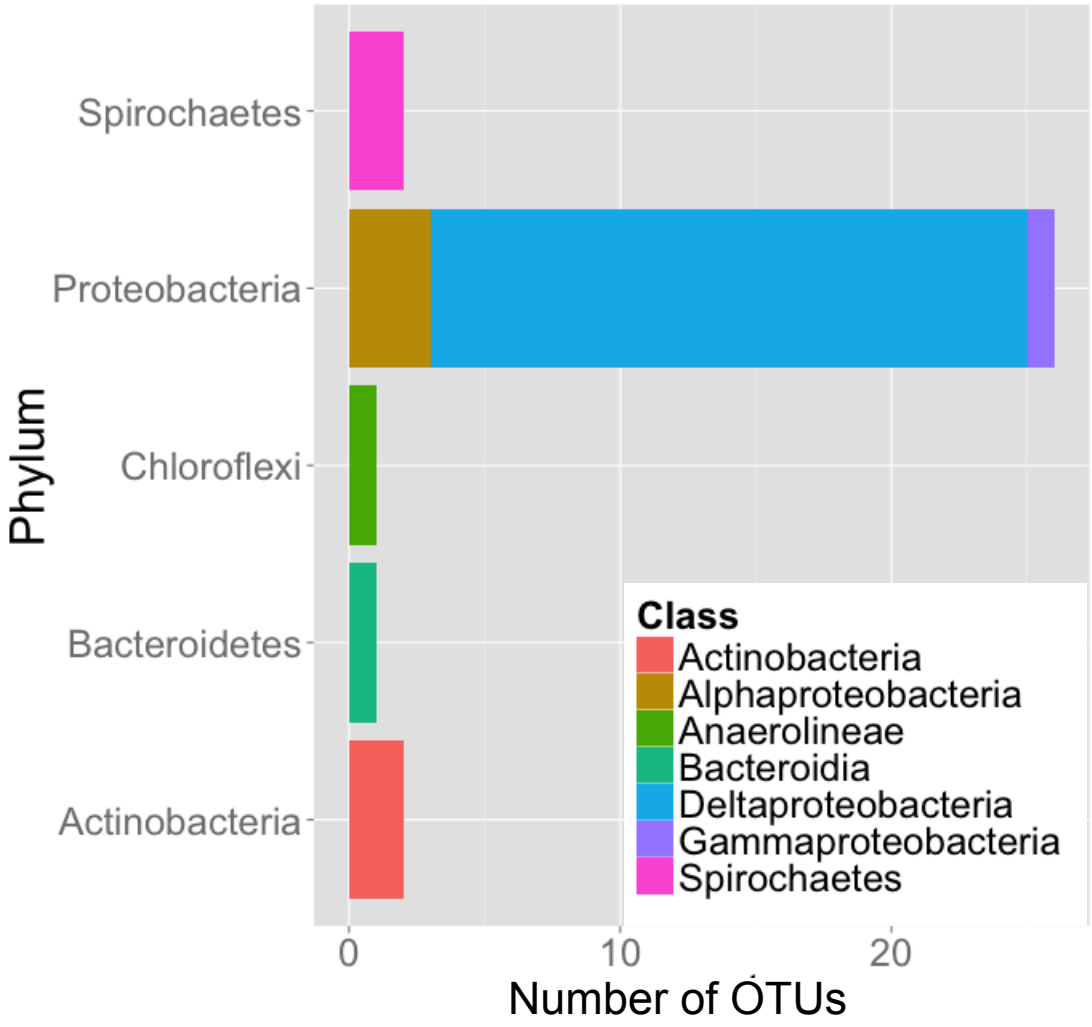

493

494 **Fig. S17. A core endospheric microbiome consisting of 32 OTUs enriched across all field**

495 **sites displayed by phylum and class.**

496

497

498

499

500

501

502

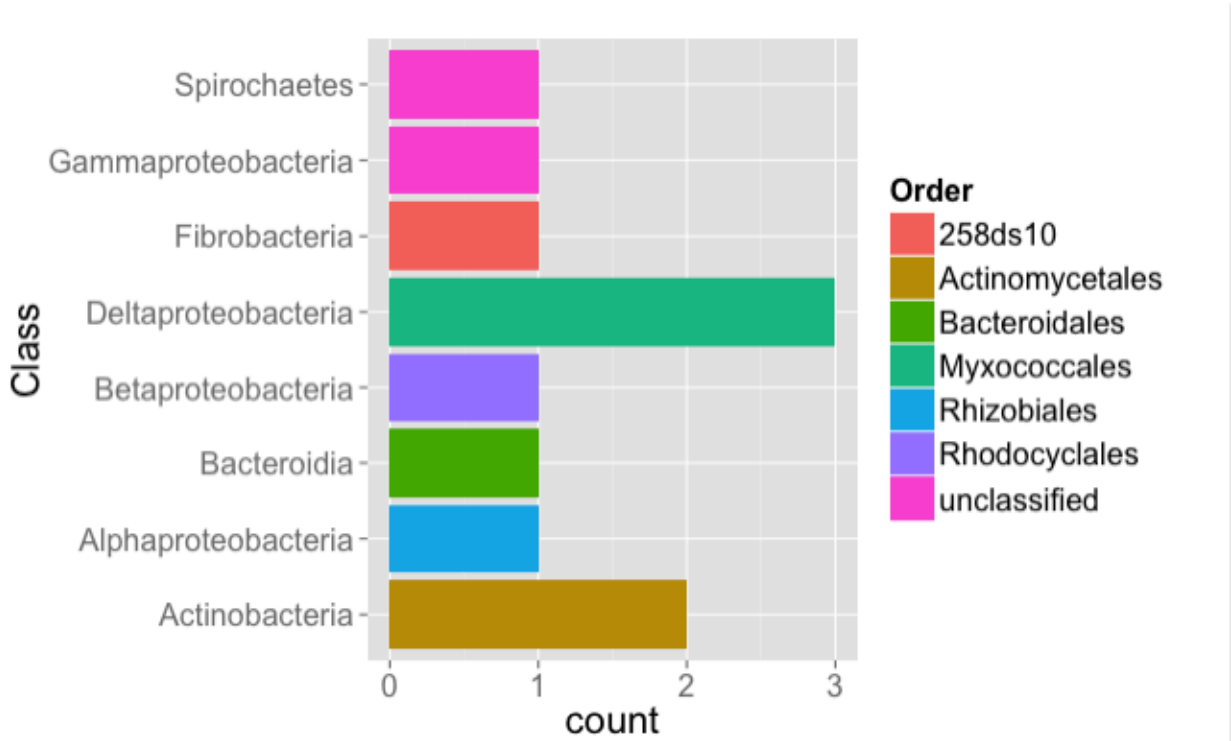

503

504 **Fig. S18 The greenhouse core endosphere enriched microbiome shares 11 OTUs with the**

505 **field enriched endosphere microbiome.**

506

507

508

509

510

511

512

513

514

515

516

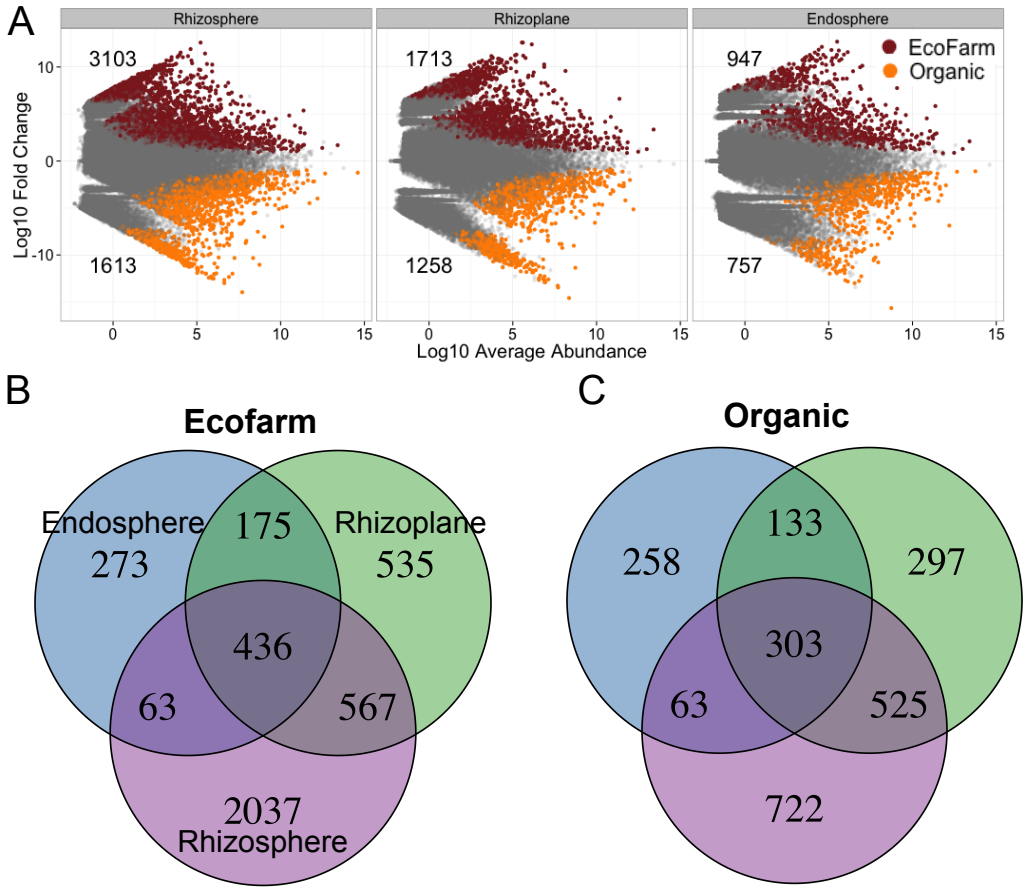

517

518 **Fig. S19. Differential OTU abundance between cultivation practices.** (**a**) MVA plot

519 displaying OTUs enriched in either organic or ecofarming practices across each

520 rhizocompartment. (**b**) Venn diagram indicating similarities of enriched OTUs between

521 rhizocompartments under ecofarm cultivation. (**c**) Venn diagram indicating similarities of

522 enriched OTUs between rhizocompartments under organic cultivation. The color scheme is

523 consistent of the rhizocompartments in the venn diagrams.

524

525

526

527

528

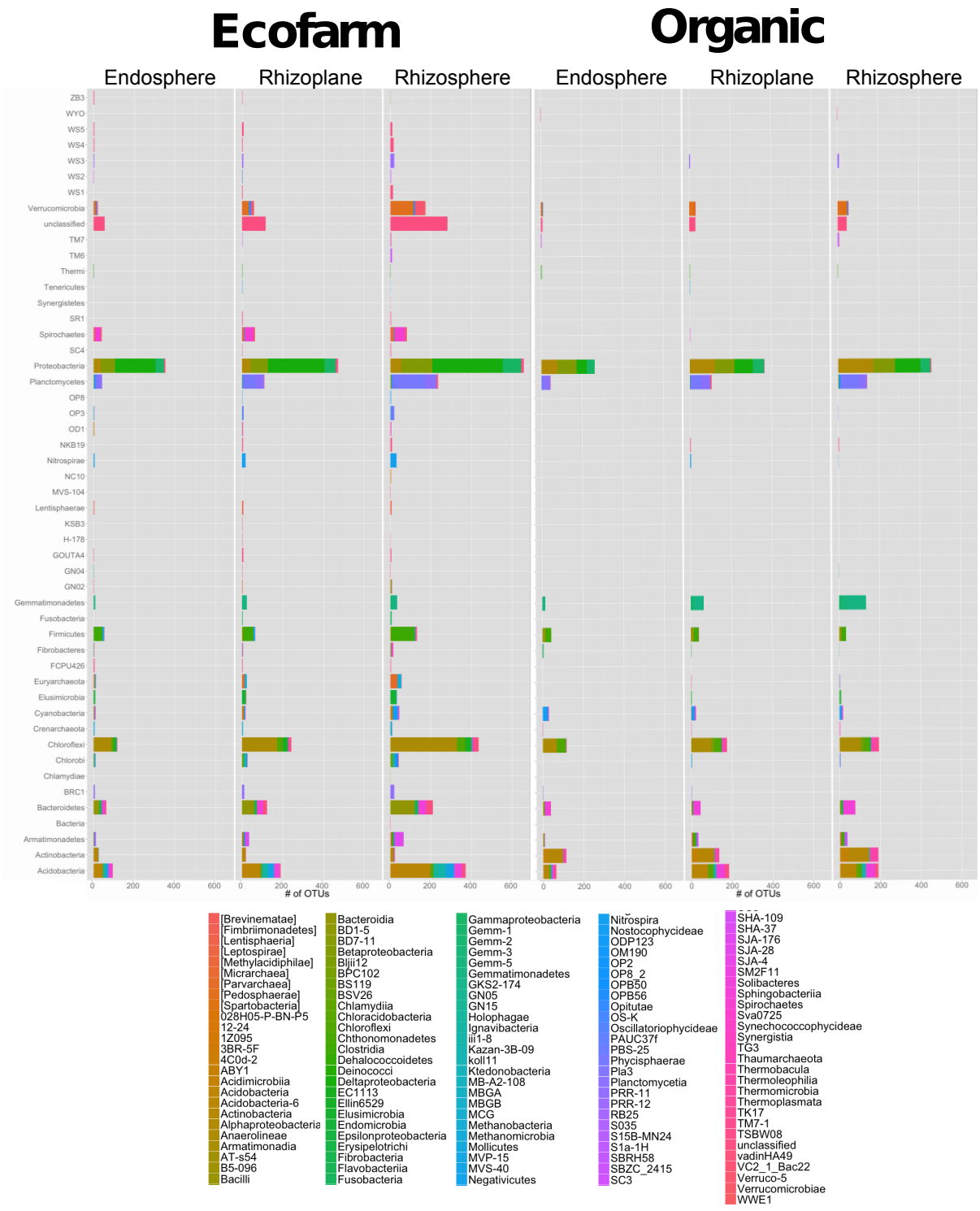

529

530 **Fig. S20. OTUs that are significantly differentially abundant between cultivation practices**

531 **mainly vary within the phyla of Proteobacteria, Acidobacteria, Actinobacteria, and**

532 **Bacteroidetes.**

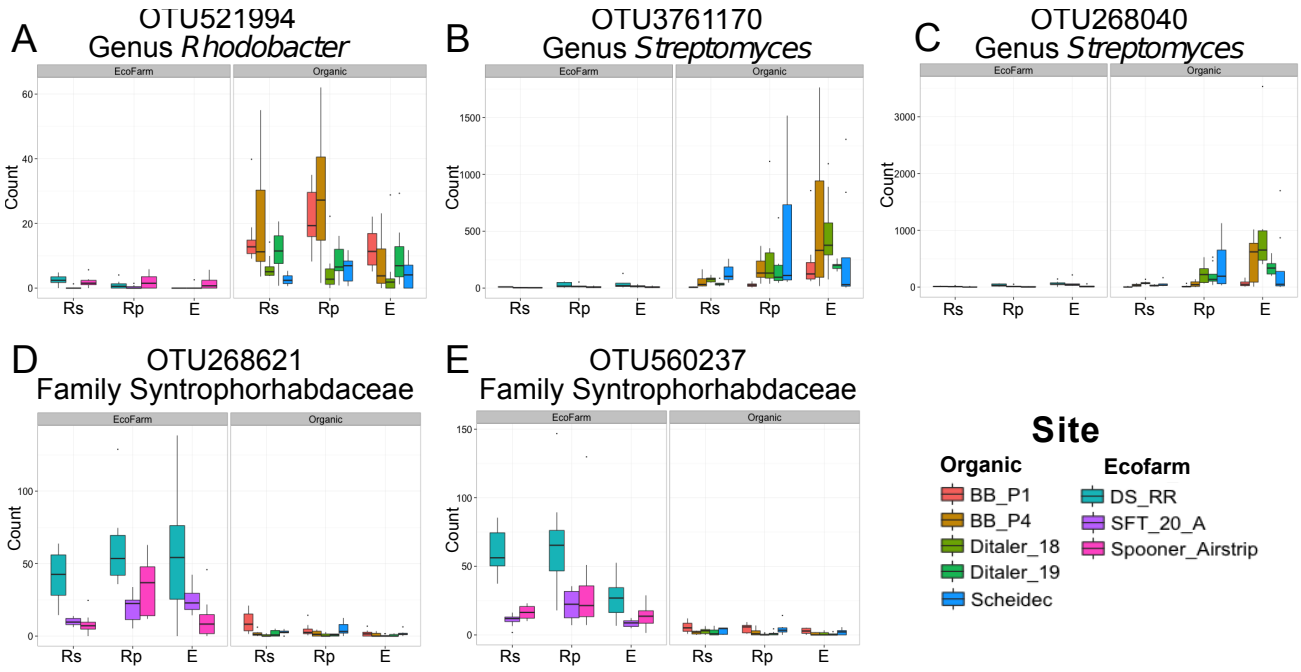

533

534 **Fig. S21. OTUs belonging to plant growth promoting rhizobacteria (PGPRs), methane**

535 **cycling bacteria, and antibiotic producing bacteria are differentially abundant under**

536 **different cultivation practices.** (**a** – **e**) Counts for OTUs separated by compartment (x-axis)

537 and field site (color).

538

539

540

541

542

543

544

545

546

547

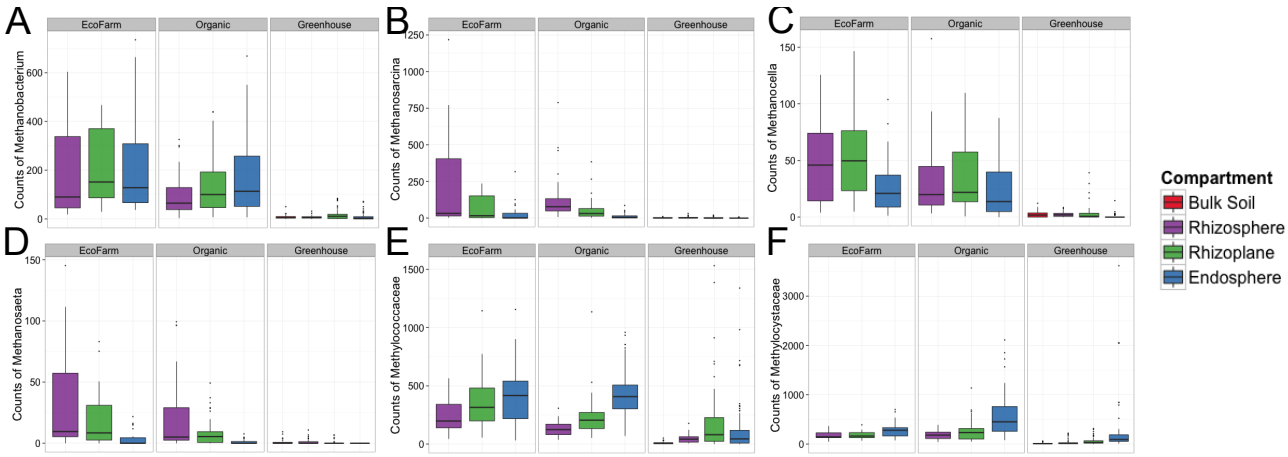

Fig. S22. OTUs involved in methane formation and oxidation have various patterns of abundance across the different rhizocompartments and growth conditions. (**a**) The sum of the abundance of all OTUs within the methanogenic genus *Methanobacterium*. (**b**) The sum of the abundance of all OTUs within them methanogenic genus *Methanosarcina*. (**c**) The sum of the abundance of all OTUs within the methanogenic genus *Methanocella*. (**d**) The sum of the abundance of all OTUs within the methanogenic genus *Methanosaeta*. (**e**) The sum of the abundance of all OTUs within the methanotrophic family Methylococcaceae. (**f**) The sum of the abundance of all OTUs within the methanotrophic family Methylocystaceae.

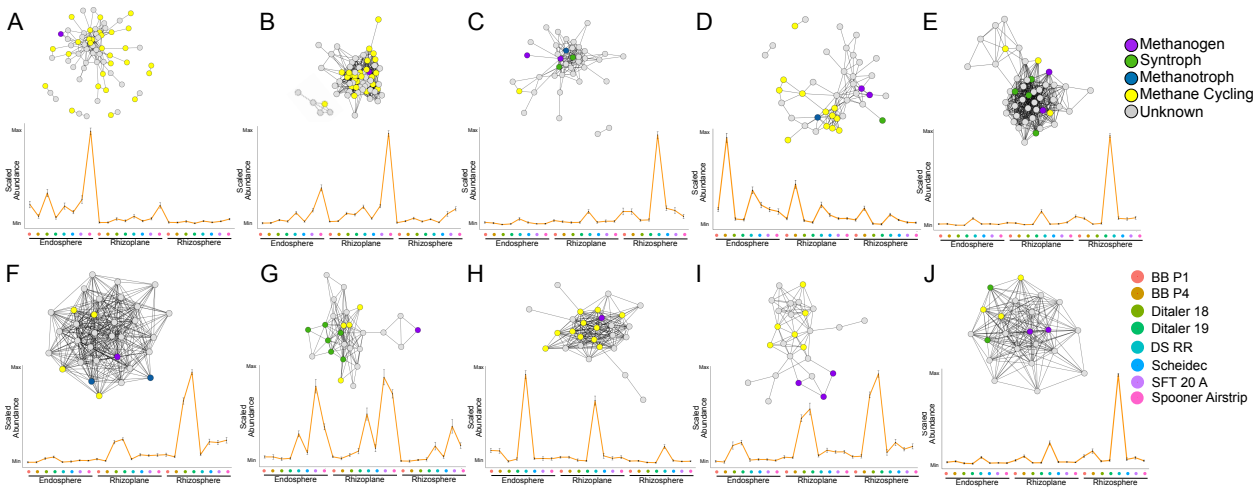

Fig. S23. Modules of the co-abundance network associated with methane cycling. Each node represents an OTU and is colored by that OTUs presumed function in methane cycling. An edge is drawn between OTUs if they have a Spearman correlation value of 0.6 or greater. (**a**) Module 6 and the average abundance profile for OTUs within the module. (**b**) Module 17 and the average abundance profile for OTUs within the module. (**c**) Module 53 and the average abundance profile for OTUs within the module. (**d**) Module 58 and the average abundance profile for OTUs within the module. (**e**) Module 75 and the average abundance profile for OTUs within the module. (**f**) Module 152 and the average abundance profile for OTUs within the module. (**g**) Module 184 and the average abundance profile for OTUs within the module. (**h**) Module 191. (**i**) Module 205 and the average abundance profile for OTUs within the module. (**j**) Module 252 and the average abundance profile for OTUs within the module. All error bars represent standard error.

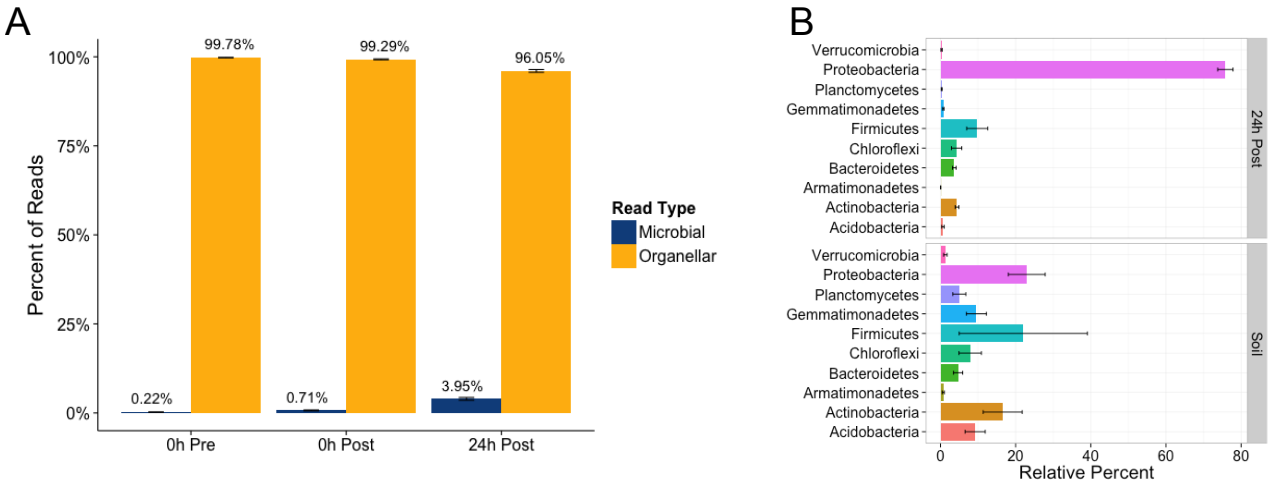

583

584 **Fig. S24 Microbe assembly into the endosphere at or before 24 hours is not a consequence**

585 **of carryover from soil contact.** (**A**) Microbe ratios in the interior of roots before transplantation

586 into soil, just after transplantation into soil, and after 24 hours in the soil. Mean percentages of

587 each read type are displayed above each bar. (**B**) Relative abundance of phyla between bulk soil

588 and 24 hours post transplantation into soil.

589

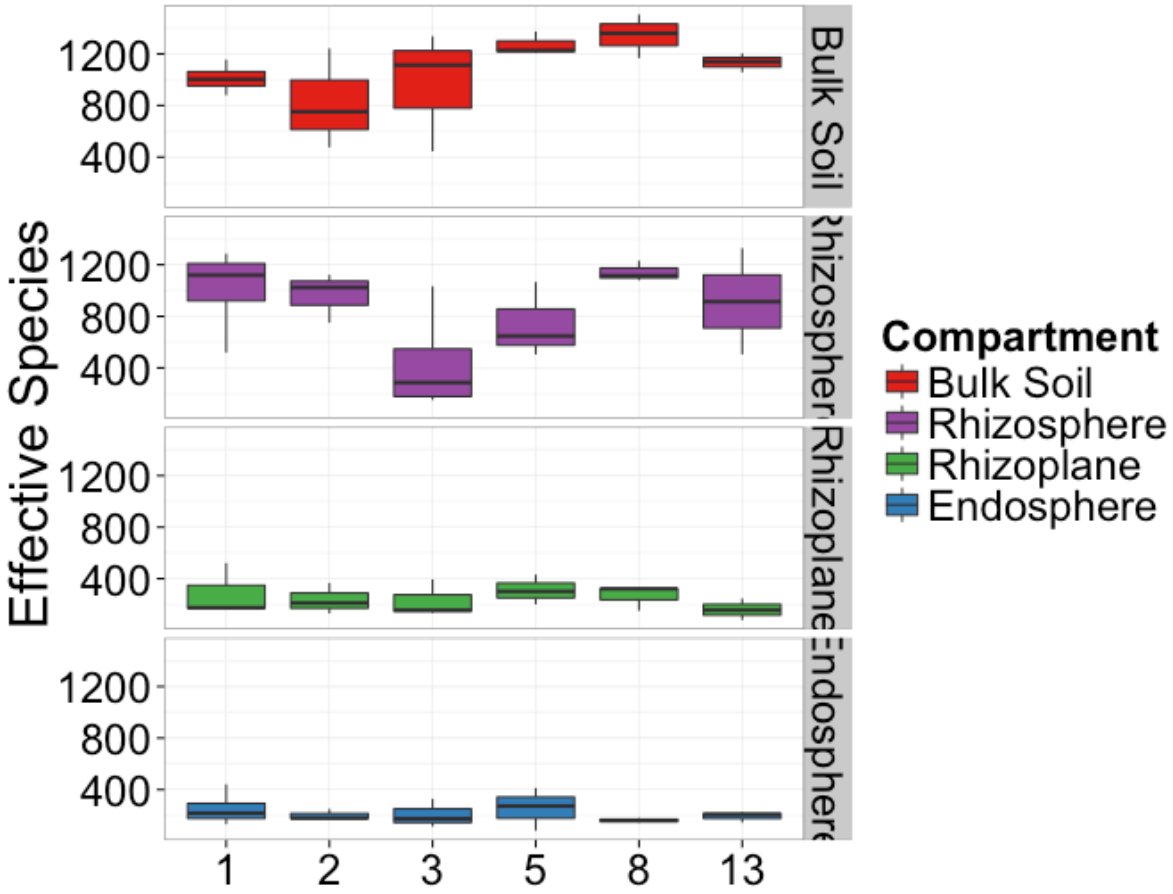

590

591 **Fig S25 Alpha diversity measurements of microbial communities in all compartments over**

592 **time.** Effective species = $e^{Shannon\_diversity}$

593

594

595

596

597

598

599

600

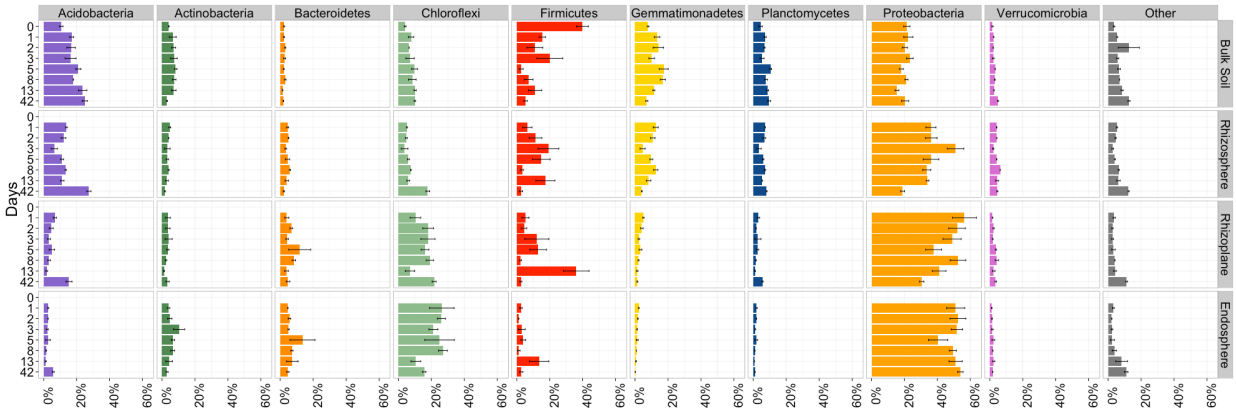

Fig. S26. There are slight shifts in the relative abundance of different phyla during the acquisition of root-associated microbiomes in each rhizocompartment.

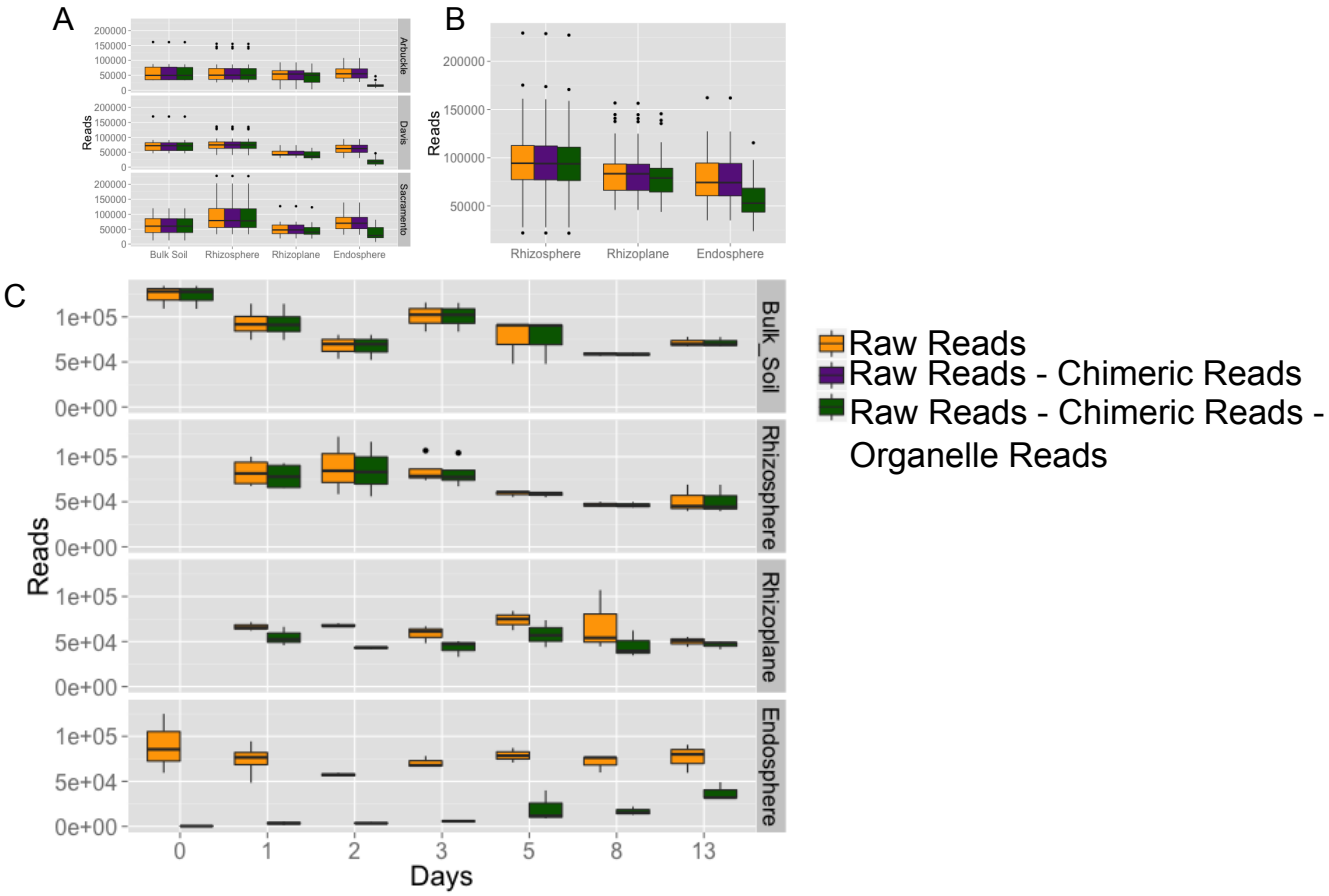

Fig. S27 Sequencing effort for each rhizocompartment in each experiment. (**A**) Greenhouse experiment. (**B**) Field Experiment. (**C**) Time series experiment. Colors represent different points in the sequence processing pipeline.

Supplementary Dataset Legends

Dataset S1. Table showing number of replicates per factor in the greenhouse and field experiment.

Dataset S2. Table displaying sequencing effort for each sample in the greenhouse experiment.

Dataset S3. ANOVA results for how various factors affect alpha diversity in the greenhouse experiment.

Dataset S4. Pairwise comparisons of alpha diversities between each compartment in each soil of the greenhouse experiment. Hypothesis testing was carried out using Wilcoxon rank sum tests and corrected for multiple testing using the Benjamini-Hochberg method.

Dataset S5. Permutational MANOVA results using weighted and unweighted UniFrac as a distance metric for the greenhouse and field experiments. (**A**) Weighted UniFrac on whole greenhouse data. (**B**) Weighted UniFrac on Greenhouse data subsetted to bulk soil and rhizosphere samples. (**C**) Weighted UniFrac on Greenhouse data subsetted to bulk soil and rhizoplane samples. (**D**) Weighted UniFrac on Greenhouse data subsetted to bulk soil and endosphere samples. (**E**) Weighted UniFrac on Greenhouse data subsetted Arbuckle samples. (**F**) Weighted UniFrac on Greenhouse data subsetted Sacramento samples. (**G**) Weighted UniFrac on Greenhouse data subsetted to Davis samples. (**H**) Unweighted UniFrac on whole greenhouse data. (**I**) Unweighted UniFrac on Greenhouse data subsetted to bulk soil and rhizosphere samples. (**J**) Unweighted UniFrac on Greenhouse data subsetted to bulk soil and rhizoplane samples. (**K**) Unweighted UniFrac on Greenhouse data subsetted to bulk soil and endosphere samples. (**L**) Unweighted UniFrac on Greenhouse data subsetted Arbuckle samples. (**M**) Unweighted UniFrac on Greenhouse data subsetted Sacramento samples. (**N**) Unweighted UniFrac on Greenhouse data subsetted to Davis samples. (**O**) Weighted UniFrac on whole Field Experiment data. (**P**) Unweighted UniFrac on whole Field Experiment data.

Dataset S6. Comparisons of phyla differential abundance between compartments in the greenhouse experiment. Hypothesis testing was carried out using Wilcoxon rank sum tests and corrected for multiple testing using the Benjamini-Hochberg method.

Dataset S7. OTUs that are significantly differentially abundant between rhizocompartments in the greenhouse experiment.

Dataset S8. Results of soil chemical analysis from the greenhouse experiment.

Dataset S9. OTUs that are significantly differentially abundant between rhizocompartments for each soil tested in the greenhouse experiment.

Dataset S10. GPS coordinate locations for all the rice fields where soil or plant material was collected.

Dataset S11. Pairwise comparisons of alpha diversities between each cultivar in each compartment in each soil.

Dataset S12. OTUs that are significantly differentially abundant in each cultivar of each rhizocompartment of each soil in the greenhouse experiment.

Dataset S13. Table displaying sequencing effort in the field experiment.

Dataset S14. Impacts of tested factors on alpha diversities in the field experiment. ANOVA results are shown along with Wilcoxon rank sum tests between cultivation practices in each compartment.

Dataset S15. Pairwise comparisons of alpha diversities between each compartment of each field site for the field experiment. Hypothesis testing was carried out using Wilcoxon rank sum tests and corrected for multiple testing using the Benjamini-Hochberg method.

Dataset S16. Comparisons of phyla differential abundance between compartments in the greenhouse experiment. Hypothesis testing was carried out using Wilcoxon rank sum tests and corrected for multiple testing using the Benjamini-Hochberg method.

Dataset S17 OTUs that are significantly differentially abundant between the rhizocompartments in each field site tested of the field experiment.

Dataset S18 OTUs that are significantly differentially abundant between cultivation practices in each rhizocompartment of the field experiment.

Dataset S19. Taxonomies that belong to clones of *mcrA* sequenced from the rhizosphere and endosphere of plants grown in the DS RR field.

Dataset S20. OTUs in the co-abundance network and the modules they are assigned to.

Dataset S21. OTUs modules containing methanogenic archaea. OTUs are labeled for their known relationships to methane cycling.

Dataset S22. Taxonomies significantly enriched (FDR <= 0.05) in OTU network modules containing the methanogenic archaea genera *Methanobacterium*, *Methanosarcina*, *Methanocella*, and *Methanosaeta*.

Dataset S23. Taxonomies significantly enriched (FDR <= 0.05) in OTU network modules containing the methanogenic archaea genera *Methanobacterium*, *Methanosarcina*, *Methanocella*, and *Methanosaeta*.

Dataset S24. Comparisons of phyla differential abundance between compartments in the timecourse experiment. Hypothesis testing was carried out using Wilcoxon rank sum tests and corrected for multiple testing using the Benjamini-Hochberg method.

Dataset S25 Sequencing primers used to amplify the 16S rRNA gene.